Development of Active Seismic Vector-Wavefield Imaging Technology for Geothermal Applications

Bob A. Hardage,
James L. Simmons, Jr.,
and Michael DeAngelo

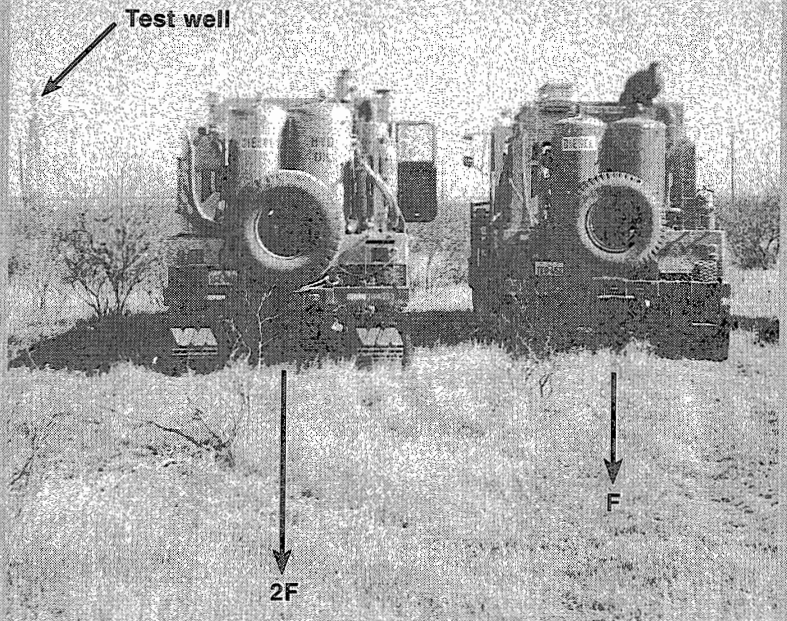

DRAFT

Final Project Report

Prepared for
U.S. Department of Energy
Idaho Operations Office
DOE

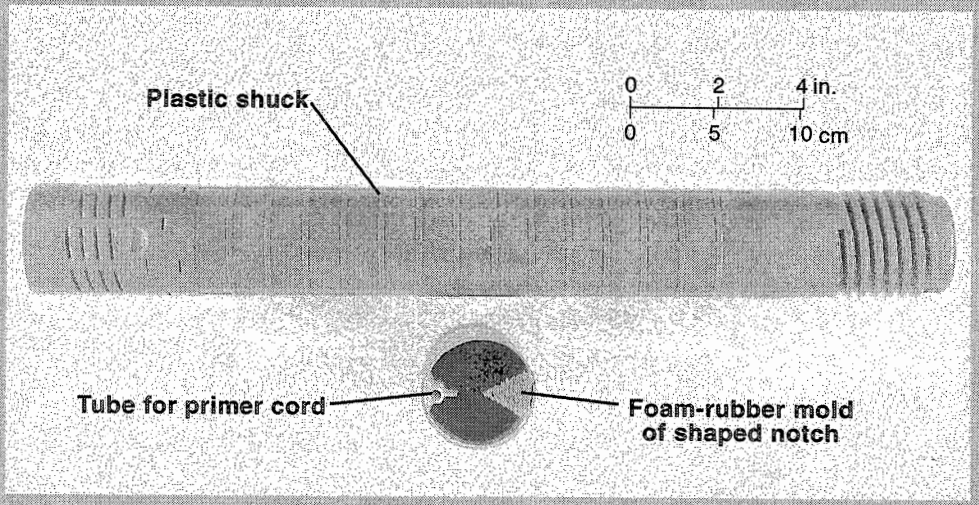

July 1999

Bureau of Economic Geology
W. L. Fisher, Director *ad interim*
The University of Texas at Austin • Austin, Texas 78713-8924

DRAFT

Final Project Report

Development of Active Seismic Vector-Wavefield Imaging Technology for Geothermal Applications

by Bob A. Hardage, James L. Simmons, Jr., and Michael DeAngelo

prepared for
U.S. Department of Energy
Idaho Operations Office

Describing work done under
Grant No. DE-FG07-97ID13573

Bureau of Economic Geology
W. L. Fisher, Director *ad interim*
The University of Texas at Austin
Austin, Texas 78713-8924

July 1999

Contents

Part II: Processing of 3-D Seismic Data over Rye Patch Geothermal Field

Figures

Abstract

This manuscript is the final report for the research project conducted under grant no. DE-FG07-97ID13573, *Development of Active Seismic Vector-Wavefield Imaging Technology for Geothermal Applications*, funded by the U.S. Department of Energy, Idaho Operations Office. The report is structured as two parts. The first, and major, portion describes the development and testing of new vector-wavefield seismic sources that can generate shear (S) waves that may be valuable in geothermal exploration and reservoir characterization. The second part describes a 3-D seismic data-processing effort to create images of Rye Patch geothermal reservoir from 3-D sign-bit data recorded over that geothermal prospect.

Vector-wavefield illumination of subsurface targets with S-waves is essential for interpreting anisotropic rock systems, particularly systems that are dominated by fractures, as many geothermal reservoirs are. Two new seismic sources were developed and tested in this study that can be used to illuminate geothermal reservoirs with S-waves. The first source was an explosive package that generates a strong, azimuth-oriented, horizontal force vector when deployed in a conventional shot hole. This vector-explosive source has never been available to industry before. The second source was a dipole formed by operating two vertical vibrators in either a force or phase imbalance. Field data are shown that document the strong S-wave modes generated by these sources.

Three-dimensional (3-D) seismic technology has had a tremendous economic influence on oil and gas exploration. Thus applications of 3-D seismic techniques may also have an economic impact on geothermal exploration and must be evaluated. One such 3-D seismic evaluation was done as the final phase of this study. Tape copies of a 3-D P-wave seismic survey (not a vector-wavefield survey) recorded in sign-bit format over Rye Patch geothermal field in northwest Nevada were received from Subsurface Exploration Company. These data were reprocessed, and the results of the data-processing research were coordinated with Lawrence Berkeley Laboratory. The sign-bit data recorded at Rye Patch had low signal-to-noise character, and the final migrated data volume had limited interpretation value. Recommendations for improving 3-D seismic data quality in future geothermal surveys are provided.

Introduction

Seismic imaging technology has been considered for geothermal prospect evaluation numerous times. However, the deployment of seismic technology in the geothermal industry has not been totally successful because of the logistical, operational, and environmental constraints that are present in many geothermal prospect areas and the low signal-to-noise (S/N) seismic conditions that are associated with the geologic settings of numerous geothermal prospects. Seismic technology developed for oil and gas applications needs to be tested and demonstrated in geothermal applications. Examples of seismic technology that need to be considered by the geothermal industry are 3-D seismic imaging and multicomponent (vector-wavefield) imaging that will provide S-wave illumination of geothermal targets. A successful transfer of these two technologies to the geothermal industry requires that seismic vector-wavefield sources first be developed that will produce usable quality S-wave data in the terrains associated with geothermal prospects.

This research project developed and evaluated two vectorized seismic-source concepts that were based on (1) directional explosive charges deployed in shallow shot holes and (2) vertical vibrators operated in both monopole and dipole modes. In the final phase of the study, we processed a 3-D, P-wave, sign-bit seismic data set that had already been recorded over Rye Patch field, a geothermal prospect in northwest Nevada. Data generated by the two vector-wavefield sources were recorded in oil/gas "wells of opportunity" provided by various sponsors of research programs at the Bureau of Economic Geology, The University of Texas at Austin. These data were generated as a series of wavetests involving vertical arrays of 3-component sensors in these wells. These multicomponent wavetest data were then analyzed to determine critical properties of the compressional (P) and S-wave modes emitted by each source.

The Rye Patch 3-D seismic data were recorded by Subsurface Exploration Company (SECO) of Pasadena, California, in a separate project involving Lawrence Berkeley Laboratory. Our objective was to reprocess the data and to offer a second opinion as to the data quality and value. The Rye Patch data were recorded using conventional vertical vibrators and single-component

vertical geophones. Thus the data provided only a P-wave illumination of subsurface targets and did not quality as vector-wavefield data, the latter being the type of seismic data needed to best evaluate anisotropic reservoir systems.

This research is important because it focuses on key issues in the geothermal industry—seismic exploration in volcanic terrains, seismic fracture detection, and reservoir mapping from surface seismic measurements. The research emphasized the development of vectorized energy sources because no significant advance of vector-wavefield imaging can be made if appropriate S-wave energy sources do not exist. The research had additional value for geothermal operators in that it evaluated one of the rare 3-D seismic data sets that exist over a geothermal field.

A critical objective of this study was to develop seismic sources that can be deployed over prospects that have difficult logistical and/or environmental constraints that prohibit the use of some conventional seismic sources. One of the research objectives at the Bureau of Economic Geology (Bureau) is to test seismic sources that can be effective generators of P and S waves over oil and gas prospects in areas of dense timber where tree-clearing is not allowed (a common permitting constraint in oil and gas prospects) and in areas of row-crop fields where only narrow source strips can be permitted from the landowner. Similar surface access and environmental restrictions exist across many geothermal prospects; thus, some of the performance criteria required of vector-wavefield sources that are used over oil/gas prospects also apply to sources that are needed to evaluate geothermal prospects.

A source option of particular interest was a special packaging of directional explosives that can be deployed in shallow shot holes. The attractiveness of this source concept is that shallow shot holes can be prepared with small portable drills that can be deployed (sometimes hand-carried) across agricultural crops with minimal damage or can be operated in dense timber without having to remove trees. The second type of vectorized source technology that was investigated was vertical vibrators operating in pairs to produce monopole and oriented-dipole sources. Neither of these source options (directional explosive charges and vertical-vibrator dipoles) are currently used in either the oil industry or in the geothermal industry to generate S-waves.

Part I: Development and Testing of Seismic Vector-Wavefield Sources

S-Wave Sources and Ground Damage Issues

Surface-based seismic S-wave sources tend to create more ground damage than do P-wave sources because they must physically shear the Earth to create a robust S-wave. Some S-wave seismic sources may in fact cause sufficient surface damage to restrict their use over some geothermal prospects. For example, the surface damage created by a single cleat underneath an early generation horizontal-vibrator pad is illustrated in Figure 1. Some horizontal vibrators have four to six such cleats per pad; thus, a single horizontal-vibrator pad can create 4 to 6 times more damage than what is shown in this photograph if this style of cleat is used. It is not unusual to record and sum 20 or more sweeps at a source station, with the vibrator pad having to be moved to a new ground location for each of these sweeps. Thus ground damage such as shown in Figure 1 can be repeated again and again across each source-station location if improper cleat design is utilized by the horizontal vibrators. After S-wave data are generated at a large number of source stations, the ground surface over the prospect may take on the appearance of a huge waffle cake. In such cases, landowners often refuse to allow such damage to their property, or they charge high permitting fees for seismic access.

Impulsive S-wave sources, such as Omnipulse and ARIS, can also create surface damage that may be similar to that portrayed in Figure 1. In some instances, gravel pads are constructed at each source point so that the repeated pounding of the inclined weight used by these impulsive sources does not create a deep depression. These gravel pads usually do reduce surface damage, but they cause data-acquisition expenses to increase because of the cost and effort required to construct the gravel pads, and some landowners object just as much to gravel piles being on their property as they do to repeated surface depressions being caused by source-pad cleats.

The surface damage shown in Figure 1 is the result of excessive cleat size being used in some horizontal-vibrator designs. An alternate cleat concept was used on the horizontal vibrators used in our field tests. These vibrators had a series of shallow ridges that extended the full width of the vibrator pad. This style cleat produces minimal ground damage (Fig. 2), and field tests confirmed

that the pad could remain in a fixed location and maintain good-quality S-wave coupling for 100 sweeps or more before having to move to a new pad location. Thus proper cleat design on the ground-contact pad can minimize ground damage when surface-based S-wave energy sources are used and can eliminate many land-access problems.

Logic for Using Vector Explosives to Generate S-Waves

One vector-wavefield source concept investigated in this project was an explosive package that could be deployed in a conventional shot hole and generate either a vertically oriented or a horizontally oriented force vector. A vertically directed force vector creates a wavefield dominated by P-waves, whereas a horizontally directed force vector produces a radiation pattern that has a strong S-wave component. By using shot-hole explosives, surface damage and inconsistent source coupling can be reduced when generating S-waves.

First, the problem of excessive ground damage is better managed because properly prepared shot holes usually create an acceptable ground disturbance, particularly if the depth of the holes is limited to about 10 ft (3 m). Rarely does a landowner object to the amount of ground damage produced by shallow shot-hole drilling, and the permitting fee that landowners demand for shallow shot holes is rarely excessive.

Second, the problem of inconsistent source wavelets is usually minimized because the energy output from shot-hole explosives is efficiently transferred to the earth regardless of variations in soil consistency. In situations where the near-surface is highly attenuating or causes excessive static problems, consistent energy transfer can be assured by drilling shot holes that extend below all, or most, of the troublesome near-surface.

An additional advantage to using shot-hole explosives is that a broader S-wave bandwidth may be achieved. Surface-generated S-wave data are notoriously narrowband (e.g., 10–30 Hz), which limits the resolution and utility of S-waves. When P-wave data generated by a surface-based source are compared with P-wave data produced by shot-hole explosives, it is often observed that

the shot-hole data have higher frequencies and a broader bandwidth. Explosive charges detonated in shot holes can sometimes generate P-wave frequencies as high as 200 Hz. Thus, the possibility of producing S-wave data with frequencies higher than those produced by surface-based sources may be realized with explosive shots that generate horizontal force vectors below the ground surface.

S-Wave Explosive Source

One S-wave source technology that offers promise is an explosive package that produces a horizontally directed force vector that is oriented in a specific azimuth direction (Fig. 3). To be commercially viable, this explosive packaging must be capable of being deployed in standard-diameter shot holes. Figure 3a is drawn to scale to represent a 4-inch-diameter (10-cm) hole having a depth of 10 ft (3 m). Shot holes can be drilled with rock bits of various sizes, but the hole diameter rarely exceeds 5 inches (13 cm). For reasons of economy, shot holes need to be as shallow as possible, yet they must be deep enough to ensure that there is an optimal transfer of explosive energy to the earth and that no rifling effect occurs at the surface. Shot holes will rarely be shallower than the 10-ft (3-m) depth implied in Figure 3; they may often be as deep as 20 to 60 ft (6 to 18 m) or more to ensure that optimal energy coupling is achieved.

Source Requirements

The critical requirement of any explosive packaging used for seismic vector-wavefield imaging is that the output force vector must be capable of being oriented in a specified horizontal direction so that it creates a robust, polarized, horizontal shear impulse to the earth (Fig. 3b). Any force vector component that is non-horizontal will produce an increased proportion of P-wave energy, which is less desirable. Packaging concepts that could create a horizontal force vector could be some type of vertical stack of shaped charges (Fig. 4a), or a vertical stack of directional

charges (Fig. 4b), or a binary liquid explosive in a container that is molded to create a horizontally directed shaped charge (Fig. 4c).

In addition to the requirement that the output force vector be horizontal, the force vector must also be oriented in a specific azimuth direction, as illustrated in Figure 3b. This requirement that the source should create an earth impulse that is oriented in a specific azimuth direction is critical to seismic S-wave data acquisition.

Shot-Hole Diameter

Shot holes can be drilled with a variety of bit sizes, with the maximum bit diameter being controlled by the power and size of the drill rig. Truck-mounted rigs can drill holes with a bit diameter as large as 12 or 15 inches; many buggy drills are limited to bits of 6-inch diameter or less; and light, portable drills often cannot use bits with a diameter larger than 4 inches.

Even though a wide range of shot-hole diameters can be drilled, there are economic constraints that cause large-diameter shot holes to be impractical. Drilling costs increase significantly when the bit size exceeds 4 3/4 inches. At this time (1999), competitive bids for shot-hole drilling and loading average $1.50 per foot in the United States if the bit size is 4 or 4 3/4 inches but increase to an average of about $2.50 per foot if a 6-inch diameter bit is used. This increase in price (almost a factor of 2) is due to the greater cost, shorter worklife, and slower penetration rate of 6-inch bits as compared with 4 3/4-inch (or 4-inch) bits.

Applying the philosophy, "keep the cost low so there will be wider commercial use," to the shot-hole requirements for any new S-wave explosive packaging leads to the decision that shot holes used for S-wave explosive sources should have a diameter of 4 or 4 3/4 inches.

Requiring an S-wave explosive package to fit in a 4-inch-diameter shot hole will ensure that this new S-wave source technology will have the widest possible use because large shot-hole rigs capable of drilling large-diameter holes cannot be deployed in some prospect areas, for example in dense timber where no tree-clearing is allowed. In agricultural areas, there are certain calendar

periods when landowners may consent to a small, portable drill rig being used in cultivated fields but will not approve the use of a large rig. Other examples could be cited, but the basic design objective is that by insisting that this S-wave source technology work in a 4-inch-diameter hole, then industry can make the transition from standard shot-hole seismic practice to a new, vector-wavefield, shot-hole source with minimal increase in cost and can also be assured that this S-wave explosive source technology can be used in most seismic-permitting conditions.

Explosive Packaging

Package Length

To make explosive S-wave sources more economically appealing to industry, shot-hole depths should be limited to 10 ft or less whenever possible. Thus the idea of using a cardboard (or plastic) cylinder 10 ft long as an integral part of the explosive package is attractive. Such a package can be deployed easily and then azimuthally oriented in a 10-ft shot hole, which are two critical field operational requirements that must be done quickly and accurately to make a vector-explosive source technology attractive. The explosive package itself should be no longer than 24 to 30 inches. The use of a 10-ft cardboard tube for orienting the downhole explosive package is shown later in Figures 10 through 12.

Package Diameter

On the basis of the economic requirement that a shot-hole diameter be either 4 or 4 3/4 inches, the diameter of the cylinder in which the explosives are packaged should be no larger than 3 inches. This package size will allow a shaped charge to be inserted inside the cylinder and still have a modest standoff distance between the charge and the shot-hole wall (Fig. 5).

Standoff

Conventional thinking is that a shaped charge creates a narrower and deeper hole in a target and, by inference, a more directionally oriented force vector, if the standoff distance between the charge and the target (the shot-hole wall in this application) is on the order of 3 to 4 charge diameters (private communication, Austin Powder Company). The shot-hole and explosive package diameters proposed here do not create this ideal standoff geometry of 3 to 4 charge thicknesses. However, a standoff of 1.0 to 1.5 charge thicknesses can be created if the explosive package can be placed against the wall of the shot hole that is directly opposite the point where the force vector is to be applied (Fig. 5). This standoff geometry enhances the directionality of the output force and may be a critical factor in ensuring that the explosive design creates a polarized S-wave source.

Package Durability

Once shot holes are loaded, it may be several weeks before the explosive can be detonated because of weather delays or logistical, permitting, and technical problems related to the deployment of the seismic crew. The explosive package must be engineered so that the various hostile conditions that exist in typical shot-hole environments do not adversely affect explosive behavior for a period of 2 to 3 months after the explosive package is deployed and the hole is backfilled. For shaped charges, a key requirement would be that water never enter into the shaped-charge cavity during this extended stand-by time, because any solid medium (non-air) that fills the force-focusing cavity degrades the energy output and has unknown effects on the directionality of the output force vector. Downhole durability of the charges and of the explosive packaging is critical to the success of this new S-wave source technology.

Cavity Seal

One of the critical parameters of a shaped charge is the cavity that focuses the output force vector. The apex angle of a cavity ranges from 45° to 90° typically; a 60° angle is shown in Figure 5. For a shaped charge to function properly, this cavity must be air filled. If water or soil fills the cavity, the focusing capability of the charge is impaired, and a properly polarized output force vector may not be generated. Thus, for a shaped charge to function properly in a shot hole, there must be a durable, waterproof seal across the cavity face (Fig. 5).

Austin Powder Alliance

A technical alliance was established between the Bureau and Austin Powder, a major supplier of explosive products to the construction, mining, and seismic industries, to develop and test vector-explosive technology. The basic packaging concept was agreed to be a cylindrical charge, 6 to 24 inches (15 to 50 cm) long, with a shaped notch extending the complete length of the explosive. Two explosive materials and two package constructions were tested in this study:

- a short, 6-inch (15-cm) cast of high-density, high-velocity pentolite (a mixture of pentaerythritol tetranitrate and trinitrotoluene), and
- a long, 24-inch (60-cm) plastic tube filled with a low-density, low-velocity emulsion (the exact chemistry of this emulsion is proprietary to Austin Powder).

Photographs of these explosives will be shown later to clarify these word descriptions. The terms high-velocity and low-velocity are relative, but in this report, *high-velocity* will be used to describe an explosive that has a velocity of detonation (VOD) that exceeds 22,000 ft/s, and *low-velocity* will refer to explosives that have a VOD less than 12,000 ft/s.

Physics of Shaped Charges

The basic design of the shaped charges developed and tested in this program is illustrated in Figures 6 and 7. Figure 6 is a vertical view looking down on one of the cylindrical packages to show the interaction between the propagating shock front and the shaped-charge notch at various stages of detonation. In this perspective, the shock front begins to approximate a plane wave as it approaches the apex of the shaped-charge notch (Fig. 6b).

As the quasi-plane wave sweeps past the notch (Fig. 6c), it creates force vectors F_1 and F_2 that are normal to notch faces OA and OB, respectively. The components of F_1 and F_2 that are perpendicular to line OC cancel each other because they act in opposite directions. The components that are parallel to OC add constructively to create a strong horizontal force vector **F** oriented in the direction of line OC.

The behavior of the detonation front in section view is depicted in Figure 7. In this animation, the VOD in the igniter cord is assumed to be three times greater than the VOD in the explosive material, which is the VOD ratio used in explosive design number 2 that will be discussed later. The charge length of 24 inches used in the illustration is approximately the length of the final design package developed in this investigation. Thus when the igniter cord has burned 24 inches, the detonation front has progressed only 8 inches (full detonation panel) in the explosive material. The force vector **F** is the same vector shown in Figure 6.

Vector-Explosive Concept 1: Cast Pentolite

The first vector-explosive concept fabricated by Austin Powder for this research investigation was a shaped charge of pentolite. Pentolite can have a range of bulk density and VOD values, depending on the percentages of pentaerythritol tetranitrate and trinitrotoluene used to fabricate the material. The particular formulation used for the vector-wavefield explosive had a bulk density of 1.6 gm/cm^3 (approximately) and a VOD of 23,000 ft/s (7,000 m/s).

Pentolite is a solid at room temperature. To fabricate the material as a shaped charge, it is melted in a steam-heated kettle and poured into molds. The molds used to fabricate the explosives used in this vector-wavefield testing program created explosive packages 6 inches (15 cm) long with a diameter of 1.5 inches (3.8 cm). Charges were made with three different angles, 45°, 60°, and 90°, in the notch that extended the length of the explosive package.

Steel Plate Deformation Tests of Directionality

To demonstrate the horizontal directionality of the output force vector generated by the pentolite shaped charges, test charges were enclosed with 0.5-inch (1.25-cm) steel plates that were held in place with plastic tie strips (Fig. 8). This encased charge was then buried about 2 ft (60 cm) deep in sand and detonated. Comparing the relative deformations for the steel plates that were in front of, in back of, below, and above the shaped-charge notch provided a qualitative measure of the directionality of the output force vectors generated by the charge. An example of one of these steel-plate-deformation tests of directionality is shown in Figure 8. In all tests, the plate in front of the shaped-charge notch was more deformed that were any other plates, implying that the dominant force vector was oriented in the direction that the notch was facing. When these cylindrical charges are deployed vertically in a shot hole with the shaped-charge notch facing in a selected horizontal direction, the charge should generate a horizontal force vector in the direction that the notch is facing and create a stronger S-wave response then does a conventional seismic explosive.

Field Test: Bee County, Texas

The pentolite-based shaped charge shown in Figure 8 was tested in a vertical wavetest performed in a well of opportunity in Bee County, Texas. This test was disappointing in that the S-wave content of the wavefield generated by the shaped charge was not significantly different from the S-wave component of the wavefield produced by a standard seismic charge. Conditions that perhaps contributed to this unexpected behavior of the shaped-charge explosive were that

logistical constraints required that the shot holes be drilled with a 10-inch auger rather than a 4-inch drill bit, and that these large-diameter holes could not be properly backfilled with the large, hardened clay clods produced by the auger in the soil conditions that existed at this site. The large standoff distance between the shaped charge and the shot-hole wall evidently did not allow an effective shear impulse to be created (Fig. 9). The shortcomings of this test resulted in decisions never to deviate from standard size (4- to 5-inch-diameter) shot-hole drill bits, regardless of field logistical problems, and to redesign the explosive package as described in the following section.

Vector-Explosive Concept 2: Low-Velocity Emulsion

Two criteria dictated the design of the second vector-wavefield explosive package, these being (1) the package length should be increased to 2 ft or more, and (2) the VOD of the explosive should be as low as possible. The logic behind these design criteria was that they would cause the explosive to create a force vector that was a better approximation of the force vector created by the pads of established S-wave energy sources such as horizontal vibrators, Omnipulse units, and Aris vehicles. The width of the pads of these sources is of the order of 3 to 4 ft; thus, the length of the explosive should be at least 2 ft to approximate the dimension of the earth to which a shearing force is applied. The impulse motions of Omnipulse and Aris pads occur over a time period on the order of 1 ms or more; thus the VOD of the explosive needs to be low to cause the explosive force vector to be applied to the earth for a longer time interval.

These objectives resulted in a design that used a plastic shuck package that was 26 inches long and had a diameter of 3 inches. The explosive was a non-rigid emulsion having a VOD of approximately 8,000 ft/s. A lower VOD was not possible because a VOD of 8,000 ft/s is about the lowest VOD that can sustain an effective shock front. A 90° shaped-charge notch was created by taping a 26-inch length of plastic dry-wall corner strip to the interior of the plastic shuck before filling the shuck with the soft emulsion. A PETN igniter cord having a VOD of approximately 25,000 ft/s was inserted along the complete length of the package at a circumference position

directly opposite the shaped-charge notch (Figs. 6 and 7). Photographs of this package concept being assembled and deployed in the field are shown as Figures 10 through 12.

Field Test: Mercer County, Pennsylvania

The first vertical wavetest of the low-velocity-emulsion shaped charge package was done in Mercer County, Pennsylvania. The field geometry involved in the test is illustrated in Figure 13. The test well where vector-wavefield explosive data were recorded was a VSP well of opportunity that became available through a separate Bureau research project.

The key data acquired in this test are illustrated in Figure 14. The data in Figure 14a were recorded with vertically oriented downhole geophones and show a robust P-wave first arrival and no S-wave arrivals. The data in Figure 14b were recorded with horizontally oriented geophones and show a robust S-wave, implying that the S-wave motion is more of an SH nature than SV. The principal conclusion of the test results was that this second package design was a more effective S-wave energy source than the cast pentolite concept used in the first field test in Bee County, Texas.

Field Test: Stephens County, Oklahoma

A vertical wavetest of the low-velocity-emulsion shaped charge was done in a second well of opportunity in Stephens County, Oklahoma. This wavetest was important because it provided a direct comparison with wavefields generated by horizontal vibrators and with wavefields produced by vertical-vibrator dipoles. A 5-level array of wall-clamped, 3-component geophones was provided by Western Atlas (now Baker Atlas) to record the downhole wavefields. Horizontal vibrators, dipole and monopole configurations of vertical vibrators, and shot holes loaded with vector explosives were positioned at several offset locations away from the receiver well as shown in Figure 15.

This particular well of opportunity turned out not to be the best choice for a vertical wavetest because there was poor casing-to-formation coupling over most of the well bore. Unfortunately, casing-to-formation coupling can be tested only by attempting to record downhole data, not by pre-test analysis of well data. Satisfactory geophone coupling did exist in the depth range between 8,500 and 8,850 ft, and we made source comparisons using wavefields recorded only in this restricted receiver-station interval.

A comparison of the downgoing S-waves generated by horizontal vibrators and by vector explosives is shown in Figure 16. The horizontal-vibrator data were generated by two side-by-side vibrators weighing 54,000 lb. The sweep range was 6 to 48 Hz; the sweep length was 16 s; the sweep rate was linear. The vector-explosive data were generated by detonating a single 2-lb low-velocity-emulsion package (Figs. 10 through 12) at a depth of 10 ft. Vector-explosive traces are omitted at some receiver stations because the data recorded at those stations were unacceptably noisy because of poor coupling of the horizontal geophones. The S-wave illumination created by these special explosive packages has a lower energy level than the S-wave illumination produced by the horizontal vibrators. This difference in energy level is not a great concern, because the amplitudes of the explosive-generated S-waves can be amplified by increasing the charge size or the number of shot holes in the array.

Commercial Package Design

The explosive packages shown in Figures 10 and 11 are handmade products, not commercial, mass-produced units. Once test data confirmed that the second package design was effective, Austin Powder developed a packaging concept that would allow mass production of the shaped charges.

The package design of the commercial product is illustrated in Figure 12b. This design utilizes only one cylindrical plastic shuck. The physical constraint that forces the non-rigid emulsion to maintain a shaped-charge notch is accomplished by a triangular strip of high-porosity plastic foam

that is secured along the entire length of the inner wall of the shuck. This foam creates an air-filled notch, which creates the desired shaped-charge effect. A hollow tube is secured along the entire length of the inner wall of the shuck directly opposite from the foam notch to house the high-velocity pentolite cord that ignites the low-VOD emulsion.

This design provides the basic technical requirements for the vector-explosive source: low-VOD explosive material, shaped charge with a horizontal force output, and an air-filled notch cavity. The design is also an attractive package from a manufacturing cost perspective.

Vibrator-Dipole S-Wave Source

The second vector-wavefield source concept investigated in this study was to operate vertical vibrators in pairs to form dipole sources that generate more S-wave energy than do conventional vertical vibrators. The specific manner in which these vertical vibrators are deployed will be explained in the next section, but before the concept is described, we wish to emphasize that a dipole configuration of vertical vibrators may overcome some of the surface damage and inconsistent source coupling problems associated with other S-wave sources.

First, the problem of excessive ground damage is reduced because vertical vibrator pads create minimal ground depressions. Rarely does a landowner object to the amount of ground damage produced by vertical vibrators, and the permitting fee that landowners demand for the use of such vibrators is usually the lowest amount charged for any type of seismic source.

Second, the problem of inconsistent source wavelets is minimized because modern vertical vibrators have ground-force-phase-locking control systems that ensure that a consistent vertical ground-force function (i.e., wavelet) is created at each source station by each vibrator in a source array, regardless of what variations in soil consistency exist underneath each vibrator pad. This remarkable electronic/hydraulic control system is the main reason that vibroseis data quality and bandwidth have dramatically increased in the past decade. In contrast, ground-force-phase-locking control can be more difficult with horizontal vibrators because the fundamental assumption of

ground-force-phase-locking (that the vibrator pad and the ground are welded together for the entire vibrator sweep) may sometimes be violated in horizontal-pad motion. As a consequence, some horizontal vibrators can create an unknown ground-force function at each source station, and S-wave data quality may deteriorate because each S-wave field record has a different basic wavelet.

An additional advantage to using vertical vibrators in a dipole configuration could be that a broader S-wave bandwidth may be achieved than is possible with horizontal vibrators. Surface-generated S-wave data are notoriously narrowband (e.g., 10 to 30 Hz), which limits the resolution and utility of S-waves. Vertical vibrators can, however, phase lock to a predefined ground-force function at frequencies as high as 150 Hz. Thus, the possibility of producing broadband S-wave data may be realized by resorting to vertical-vibrator dipoles to generate S wavefields.

Monopole/Dipole Vibrator Concept

A vertical vibrator creates a ground-force vector that is oriented vertically downward at the center of its pad. In concept, a vibrator weighing 50,000 lb can generate a maximum force vector of 50,000 lb. In practice, vibrators are operated at a reduced drive level, a typical value being 80-percent, meaning that a 50,000-lb vibrator operating at this level will produce a ground force of 40,000 lb.

If two vertical vibrators are positioned a distance L apart and both vibrators create identical force vectors, they form a monopole source of dimension L (Fig. 17). As will be shown, the wavefield propagating away from a monopole source contains a surprisingly large amount of S-wave energy as well as the expected strong P-wave radiation. In contrast, if two side-by-side vibrators create significantly different force vectors, they form a dipole source of length L (Fig. 17). By definition, a dipole source generates a strong S-wave radiation pattern. A key part of this vector-wavefield source research program was based on the idea of deploying vertical vibrators in pairs, then causing each vibrator of a vibrator-pair to produce a different instantaneous ground-force magnitude, and thereby to create a series of dipole sources. Such a dipole source

should be able to illuminate geothermal targets with robust S-waves without causing excessive ground-surface damage.

Force-Controlled Dipole

Vertical vibrators, when operated in pairs, can be made to function as either a monopole source or a dipole source (Fig. 17). In dipole mode, the vibrators generate a high proportion of S-wave energy and a low proportion of P-wave energy. To properly implement S-wave seismic imaging, the polarity of the downgoing illuminating S-wavefield produced by a dipole configuration of vibrators must be a parameter that can be controlled. S-wave polarity produced by a vertical vibrator-pair operating in phase-locked mode will be defined as being either positive or negative, depending on which vibrator in the pair generates the greater magnitude of ground force. This polarity concept is illustrated in Figure 18a and c and is defined as *force-controlled dipole polarity*. It is assumed that the azimuth direction in which the S-wave particle-velocity vector points can be controlled by causing the vibrator-pair to align in different azimuth directions.

Phase-Controlled Dipole

Dipole polarity can also be adjusted to be either positive or negative by causing the phase of the applied forces across a source array to vary by 180°. For example, positive polarity might be defined as having the pad motion of vibrator 1 be 180° ahead of the pad motion of vibrator 2, and negative polarity would then be the reverse of this phase relationship. In this configuration, each vibrator in a 2-element array produces the same force magnitude, but there is an 180° phase lag between the two force vectors. This concept of *phase-controlled dipole polarity* is illustrated in Figure 18b and d.

Theoretical Vibrator Radiation Patterns

Analyses of monopole and phase-controlled dipole sources created by vertical-vibrator pairs have been published by Edelmann (1981) and Dankbaar (1983). Edelmann showed field data generated by a phase dipole; Dankbaar provided a mathematical analysis of the P and SV displacements generated by a 2-element monopole source and a phase dipole. In our study, Dankbaar's model was expanded to describe the P and SV displacements of a force dipole which were then compared with the displacement patterns produced by a phase dipole and a monopole.

Example calculations of P and SV radiation patterns are shown in Figure 19 for materials having Poisson's ratios of 0.44 and 0.33, respectively. Poisson's ratio is defined as the ratio of transverse strain to longitudinal strain. This ratio is a popular elastic constant because it conveniently relates shear wave velocity V_S and compressional wave velocity V_p through the equation,

$$\frac{V_s}{V_p} = \left[\frac{0.5 - \sigma}{1 - \sigma}\right]^{1/2}, \qquad (1)$$

where σ is Poisson's ratio. Poisson's ratio ranges from 1/2 for fluids (which have a zero value shear modulus) to 0 for perfectly rigid media that do not experience transverse strain when subjected to longitudinal stress.

The radiation patterns in Figure 19 show that a monopole source generates robust SV waves over a broad range of take-off angles (the angle measured from vertical), with the SV amplitudes being 3 to 8 times greater than P amplitudes at take-off angles of 30° to 60° (Fig. 19a, b). SV radiation lobes generated by a force dipole (Fig. 19c, d) tend to have larger take-off angles than do SV lobes generated by either a monopole or phase-dipole source. A phase-dipole (Fig. 19e, f) generates particularly robust SV amplitudes, but the SV lobes tend to be restricted to the narrowest range of take-off angles created by any of these three source options.

Vibrator-Dipole Field Tests

A total of six vertical wavetests were done at various sites to evaluate the physics of vibrator-dipole behavior. Dipole parameters that were evaluated in the first test were comparisons of data produced by dipole lengths of 12, 18, and 24 ft and by force imbalances of 1.3, 1.7, 2, and 2.5 for force-controlled dipoles. Only one phase imbalance (180°) was used for all phase-controlled dipoles. These tests led to the decision to standardize all subsequent tests to a dipole length of 12 ft and to a force imbalance of 2 for all force-controlled dipoles. Vertical vibrators positioned to form a force-controlled and a phase-controlled dipole are shown in Figures 20a and 20b, respectively. Data from two subsequent tests that utilized these dipole geometries and parameters are discussed in the following section.

Field Test: Glacier County, Montana

One of the early vibrator-dipole tests was done using a well in Cut Bank Field, Glacier County, Montana. In this test, two vertical vibrators were positioned as shown in Figure 20 to form either a monopole pair or a dipole pair. The source-receiver geometry used to generate the test data is shown in Figure 21. Data generated by vibrators operating first in monopole mode and then in dipole mode are shown for two source offsets as Figures 22 through 25, respectively. These test data have not been processed and are plotted as they were recorded. The S-wave first-arrival times are not interpreted in these displays, but a shaded strip is shown across the H2 component of the phase-dipole data (Figs. 23b and 25b) to indicate the velocity trend of a significant component of the downgoing S-wave illuminating wavefield. The S-wave first-arrival times occur one or two troughs or peaks before the times indicated by the front edge of the shaded strip for the data recorded from the 550-ft offset (Fig. 23b). The front edge of the strip in Figure 25b is probably a good approximation of the S-wave first-arrival times for the data recorded from the 1,100-ft offset.

If the downhole 3-component geophone were rotated to a consistent radial/transverse orientation at each receiver station, the SV modes could be better distinguished. However, that

coordinate rotation is not necessary in this instance because the objective of the experiment was to measure only the relative amounts of P and S energy in the radiated wavefield. Those energy measurements can be made using the unrotated data as they are displayed in these figures.

Significant S-wave energy appears on both the H1 and H2 components for each dipole source at both offsets (Figs. 23 and 25). No significant S-wave energy is evident on the vertical geophone response, implying that the downgoing S-wave from the dipoles is more SH in nature than it is SV. The S-wave component of the monopole data generated at a source offset of 550 ft (Fig. 22) is almost as energetic as the S-wave component of either dipole source (Fig. 23) when the S-wave contents of both the H1 and H2 geophones are considered. However, the S-wave content of the monopole data generated at an offset of 1,100 ft (Fig. 24) is inferior to the S-wave content of the dipole sources (Fig. 25). The general conclusion is that better S-wave illumination is achieved with a dipole source than with a monopole source. A second general conclusion is that a phase dipole appears to generate better quality S-waves than does a force dipole.

The data in Figure 23 were used to determine the P-wave velocity (V_p) and S-wave velocity (V_S) over the depth interval 2,300 to 2,950 ft. This analysis resulted in values of

$$V_p \sim 11{,}800 \text{ ft/s}$$

and

$$V_S \sim 6{,}500 \text{ ft/s},$$

leading to a V_p/V_S ratio of 1.8 for the sand-dominated lithologies in this depth range. This velocity ratio is consistent with the V_p/V_S log analyses published by Pickett (1963) and the V_p/V_S laboratory measurements made by Domenico (1984).

Field Test: Stephens County, Oklahoma

A map view of a test well in Stephens County, Oklahoma, and the offset source station locations relative to that well where test wavefields were generated is shown in Figure 26. On the basis of the results of the test in Glacier County, Montana, the only dipole source that was

evaluated in this Oklahoma project was a phase dipole. The importance of this test was that it was the first opportunity to compare the S-wave radiation pattern generated by a phase dipole with the S-wave events produced by a horizontal vibrator. Data from one source station (no. 3 in Fig. 15) recorded by downhole horizontal geophones are shown in Figure 26. These data show that a phase-dipole source produces S-wave events that are approximately equivalent to those generated by the industry's standard S-wave source, the horizontal vibrator. The data also show that there is no equivalent S-wave component in the wavefields generated by vertical vibrators operating in monopole mode (bottom panel).

A linear 16-s sweep from 6 to 48 Hz was used to generate the horizontal-vibrator data. The data shown in the top panel are a sum of eight of these sweeps from the 2-vibrator array. During a separate, year-long S-wave research program, we found that it was inadvisable to shake horizontal vibrators at frequencies above 48 Hz because of increased stress on hydraulic and mechanical systems and because of reduced energy output at higher frequencies. In contrast, the vertical vibrators that formed the phase-dipole source were swept from 8 to 64 Hz using a 12-s sweep length and a linear sweep rate. Eight sweeps from two vertical vibrators were summed to produce the phase-dipole data (middle panel) and the vertical-vibrator data (bottom panel). All data in Figure 26 were recorded with horizontal geophones.

Because of the expanded sweep bandwidth used with the vertical vibrators, there is an important difference in the frequency content of the downgoing illuminating S-waves generated by the phase-dipole and the horizontal vibrators. The time period of the S-wave first arrival produced by the horizontal vibrators is approximately 100 ms, implying that the dominant frequency of that source wavefield is 10 Hz. In contrast, the time period of the S-wave first arrival generated by the phase-dipole source is about 50 ms; thus the dominant frequency of that source is approximately 20 Hz.

This factor of 2 difference in the frequency content of the downgoing S-wave first arrivals is important for resolving thin beds and geologic detail. This test suggests that one of the potential

advantages of using vertical vibrators to form dipole sources can indeed be realized, that being that higher frequency S-waves may be generated.

Theoretical calculations of source radiation patterns imply that vertical vibrators should generate S-waves that are almost as robust as those produced by a phase dipole (Fig. 19), and reasonably robust S-waves were observed for monopole data generated at one source offset in the Montana test (Fig. 22). However, vertical vibrators produced no measurable S-wave arrivals in the wavetest geometry used in Oklahoma (Fig. 26, bottom panel).

Summary of Vector-Wavefield Source Development

We believe we have developed and demonstrated two new sources that can generate S-waves that are appropriate for evaluating geothermal prospects. The first, a vector-explosive package, has never been available to the seismic industry, and the demonstration of its source performance is considered to be a significant development.

The second source, a dipole formed by operating two vertical vibrators in either a force or phase imbalance, is a concept that has been partially analyzed by other researchers (Edelmann, 1981; Dankbaar, 1983) but has not been thoroughly tested over a variety of prospects as we have done. All previous work on vertical-vibrator dipoles has focused on phase dipoles only. We find no published work that evaluates force dipoles. We believe our work has proven that vibrator dipoles can be effective S-wave sources. Our data imply that phase dipoles appear to be more efficient S-wave sources than force dipoles.

We used the concept of vertical wavetesting to verify that these two new vector-wavefield sources are viable for full-scale field operations. We were able to do a large amount of field testing because considerable cost sharing in terms of VSP receivers, shot-hole drilling, and access to vertical vibrators, horizontal vibrators, and explosives were provided by seismic contractors. Operators also provided access to several key wells in which vertical wavetests could be done; otherwise, much of the field testing described here would not have been possible. A more rigorous

confirmation of source performance would have been to record one or more 2-D seismic lines involving all source options (vibrator dipoles, horizontal vibrators, vertical vibrators, and vector explosives). Unfortunately no budget was provided for such field work, and it was not possible to get enough cost sharing donated to the research program to record such surface profiles.

The original proposal stated that we would test and demonstrate the capability of a third S-wave source, that being a new inclined weight dropper designed to generate S-waves. This weight-dropper source was to be built and loaned to the research effort by an independent oil and gas company that sponsors research programs at the Bureau of Economic Geology. The source development was terminated by this company about half-way through the project period, when the weight-dropper source was at an 80-percent complete stage, because of the depressed economy in the oil industry. Consequently, no field tests could be done with the weight-dropper source.

Part II: Processing of 3-D Seismic Data over Rye Patch Geothermal Field

Seismic Data-Processing Objective

One of the original objectives of this project was to use 3-component geophones to acquire surface-recorded reflection data generated by the vector-wavefield sources that were tested, and then to develop data-processing algorithms that would use all three components of these vector wavefields to better remove surface-related noise modes (Rayleigh waves and Love waves) from the data. This objective had to be abandoned because the economic decline in the oil industry that occurred during the work period resulted in no industry sponsor of Bureau research being willing to pay for the field work that had to be done to record multicomponent surface reflection data. An alternative data-processing objective was then substituted, that being to process 3-D seismic data recorded over Rye Patch field in northwest Nevada (Fig. 27) by a separate geothermal research program and to share the data-processing research results with Lawrence Berkeley Laboratory.

Processing of Rye Patch 3-D Seismic Data

A 3-D seismic survey was recorded over Rye Patch geothermal field in northwest Nevada by Subsurface Exploration Company (SECO) of Pasadena, California, in 1998 (Fig. 27). This 3-D seismic data acquisition was done under the auspices of a research effort directed by Lawrence Berkeley Laboratory (LBL) and was not a formal part of the Bureau research program reported here.

These 3-D data are particularly important because they represent one of the initial attempts to infuse 3-D seismic technology into the geothermal industry. The data were recorded using vertical vibrators as sources and single-component geophones as receivers. The data are thus conventional 3-D P-wave data and not vector-wavefield data. Nonetheless, the data are important because they are one of the rare efforts to evaluate a geothermal prospect with 3-D seismic technology. The Rye Patch data presented processing challenges to the LBL scientists involved in the Rye Patch study, so the 3-D data were reprocessed as the final phase of this Bureau project to ensure that the widest

possible range of processing algorithms and strategies were applied to the data through the combined effort of LBL and Bureau researchers.

The Rye Patch data were recorded in a sign-bit format, which is a good field procedure for low signal-to-noise (S/N) data because by allowing only two possible trace amplitude values (+1 and –1), noise amplitudes are forced not to exceed signal amplitudes. SECO pre-processed the sign-bit data, created tapes of correlated field records with the field geometry in the trace headers, and then delivered these tapes to LBL and to the Bureau for data-processing research.

A map indicating the inline and crossline nomenclature used for the Rye Patch 3-D survey is provided as Figure 28. Examples of field records from the Rye Patch data are displayed as Figure 29. Each record is the response of a full receiver line chosen from typical acquisition templates. The offset distance to each receiver line increases from Figure 29a to 29d. Rarely could reflection signal be seen in any of the Rye Patch field records, which indicated the Rye Patch prospect was a poor seismic signal area. One exception to this general condition was chosen for display, that being the record in Figure 29b that has a good quality shallow reflection event.

One data-processing problem was the lack of good-quality refraction breaks over portions of numerous records, such as the situation shown for the near-offset traces in Figure 29a. A major noise problem was the occurrence of numerous secondary scatterers such as those labeled in Figures 29b and c. These secondary scattered wavefields are assumed to be caused by surface waves reflecting back to the receiver stations from local topographic relief features (Fig. 27).

We subcontracted the reprocessing of these field data to Trend Technologies of Midland, Texas. Trend has excellent 3-D seismic processing technology and extensive experience with sign-bit data and with low S/N seismic data. Because of their seismic processing expertise, Trend has been subcontracted to process several 3-D data volumes for the Bureau. In our opinion, the Rye Patch data were processed by one of the better qualified seismic data-processing shops in the oil and gas industry.

Trend, like LBL, could not create an interpretable-quality 3-D image from the Rye Patch data. Examples of inline and crossline profiles through the final stacked 3-D volumes created by Trend

are shown in Figures 30. Even though the field records had low S/N character, the poor quality of the stacked data was surprising. The lack of interpretable reflections is a concern because early disappointments about 3-D seismic technology in geothermal applications will make it difficult to justify additional 3-D seismic efforts over geothermal prospects.

Migrated versions of crossline 80 and inline 100 are displayed in Figures 31a and b. Migration tends to increase the signal-to-noise ratio by focusing reflection energy to its correct subsurface reflection points. Reflection continuity can usually be further enhanced by applying a spatial-averaging type of deconvolution to either stacked or migrated data. Both processes—migration and an FXY deconvolution—were utilized to make the data displays in Figures 31a and 31b. Although the lateral continuity of events was enhanced, the data were not considered to be of interpretable quality.

Faults are considered to be important influences on the Rye Patch structure. From past experience, it is known that faults can usually be better seen in low-quality seismic data by limiting the frequency of the data to just the first octave of the signal spectrum. Consequently, a low-pass filter was applied to the migrated data to restrict the frequency content to 8 to 16 Hz. The filtered data emphasize vertical-trending discontinuities in the data that may be indicative of faults (Figs. 31c and d). However, a fault interpretation based on these discontinuities should be done with caution because the poor quality of the stacked data (Fig. 30a, b) cause any derivative of those data to be a product of questionable value.

It may indeed be true that 3-D seismic reflection technology does not work at Rye Patch field and perhaps at many other geothermal prospects. However, before 3-D seismic imaging and vector-wavefield technology are abandoned at Rye Patch or in any other geothermal area, the following possible reasons for the poor data quality shown in Figures 30 and 31 need to be considered.

1. Geometry errors – Processors at both Trend and LBL noted that any surface-consistent algorithm applied to the Rye Patch data resulted in a degradation of data quality. Any time a surface-consistent process deteriorates 3-D seismic data quality, experience has shown

that there are almost always geometry errors associated with some of the source and/or receiver stations. Thus there is a strong possibility that geometry errors exist in the trace headers of the field tapes provided by SECO. The field-observer notes included with the tape shipment did not have enough detail to check the station geometries associated with each source template. The geometry specified in the trace headers by SECO had to be totally trusted by the data processors. It would be worthwhile to have SECO check the geometry parameters and coordinates written in the trace headers.

2. Poor quality control of field data – The sparse information in the observer's notes and the suspicion of geometry errors in the field tapes are problems that can be eliminated in future geothermal 3-D seismic programs by having an experienced field geophysicist monitor all aspects of the field work on behalf of DOE and/or the geothermal operator. A field "bird dog" is commonly assigned to all 3-D seismic programs done in the oil and gas industry just for these reasons.

3. Lack of presurvey wavetest - A comprehensive wavetest program needs to precede all future geothermal 3-D seismic efforts to determine which source parameters (bandwidth, sweep length, energy level, charge size, charge depth, array size), receiver parameters (array size, array shape, numbers of elements per string), and template geometry (line spacing, station spacing, areal dimensions) will produce optimal data quality. It is common practice to record a presurvey wavetest in oil and gas applications of 3-D seismic data to ensure that the subsequent seismic program is properly implemented, or to advise an operator that a 3-D seismic program will probably not succeed. This same practice needs to be introduced into geothermal applications of 3-D seismic data.

Summary of Data-Processing Research

The 3-D sign-bit seismic data recorded over Rye Patch field have a low signal-to-noise ratio. The fact that any surface-consistent processing effort seemed always to degrade data quality

implies that geometry errors may exist in the trace headers of the field tapes. Such errors can be verified and reconciled only by the contractor who created the field tapes that were sent to the data-processing contractors.

The final migrated data volume contains reflection events that are laterally continuous over limited portions of the 3-D image space. The discontinuities that separate these zones of coherent reflections could be interpreted as faults, but such interpretations would have to be supported by production flow tests, pressure tests, and production histories to verify that barriers to lateral fluid flow actually exist at these reflection discontinuities. Any fault interpretation based on the 3-D seismic data alone would be questionable.

References

Dankbaar, J. W. M., 1983, The wavefield generated by two vertical vibrators in phase and in counterphase: Geophysical Prospecting, v. 31, p. 873–887.

Domenico, S. N., 1984, Rock lithology and porosity determination from shear and compressional wave velocity: Geophysics, v. 49, p. 1188–1195.

Edelmann, H. A. K., 1981, Shover shear-wave generation by vibration orthogonal to the polarization: Geophysical Prospecting, v. 29, p. 541–549.

Pickett, G. R., 1963, Acoustic character logs and their application in formation evaluation: Journal of Petroleum Technology, p. 659–667.

Fig. 1. Surface damage caused by a single cleat of an early-generation horizontal vibrator after executing one source sweep. The arrow shows the direction of cleat movement, This pyramid-shaped hole is approximately 15 in (38 cm) deep, 18 in (46 cm) wide, and 24 in (61 cm) long. A man's cap is shown in the hole for scale. A small portion of the indentation caused by a neighboring cleat can be seen at the bottom of the photo.

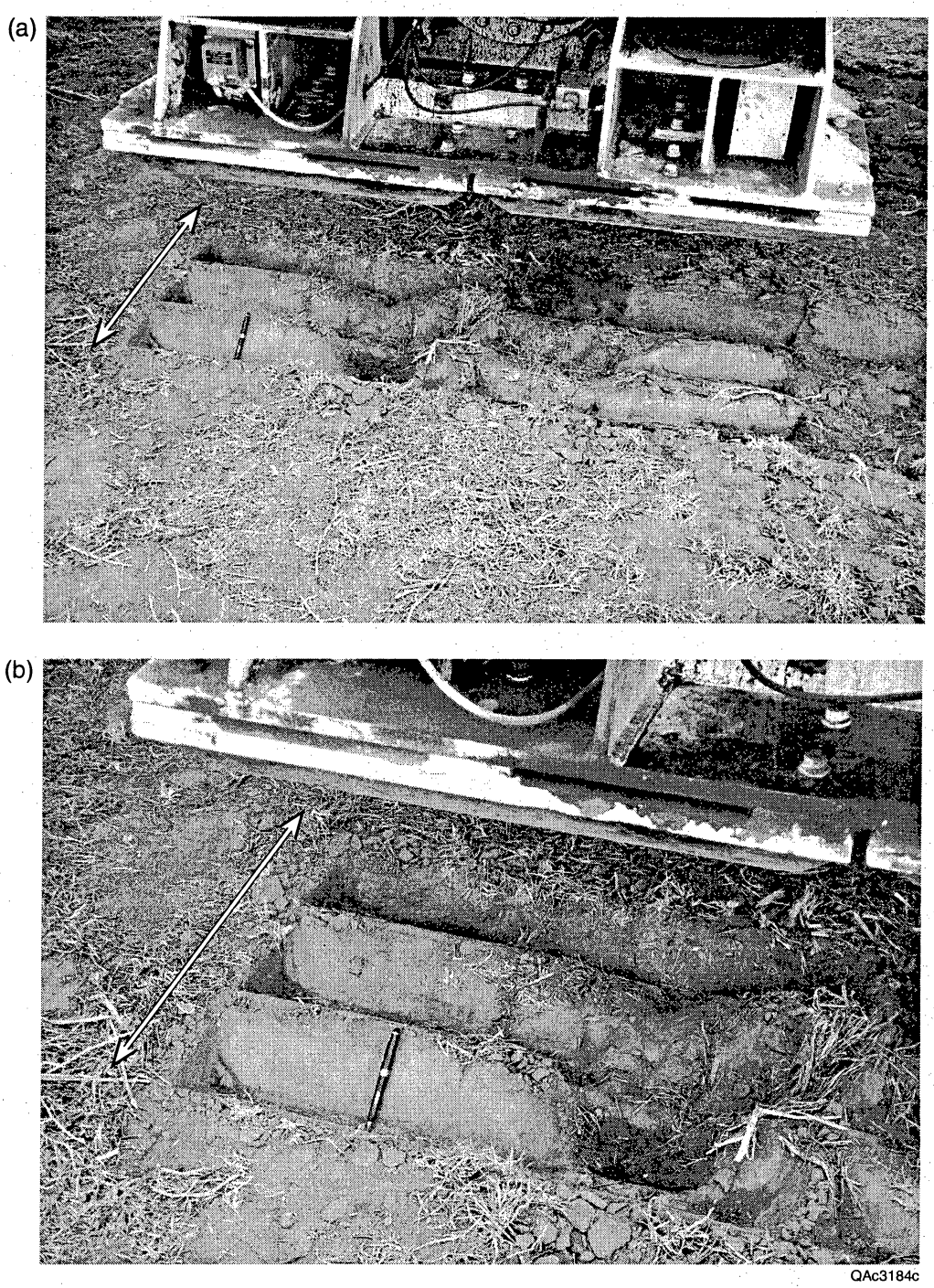

Fig. 2. (a) Minimal damage caused by a horizontal vibrator with a properly designed base cleat. The arrow shows the direction of pad motion. A writing pen is shown for scale. (b) Zoom view.

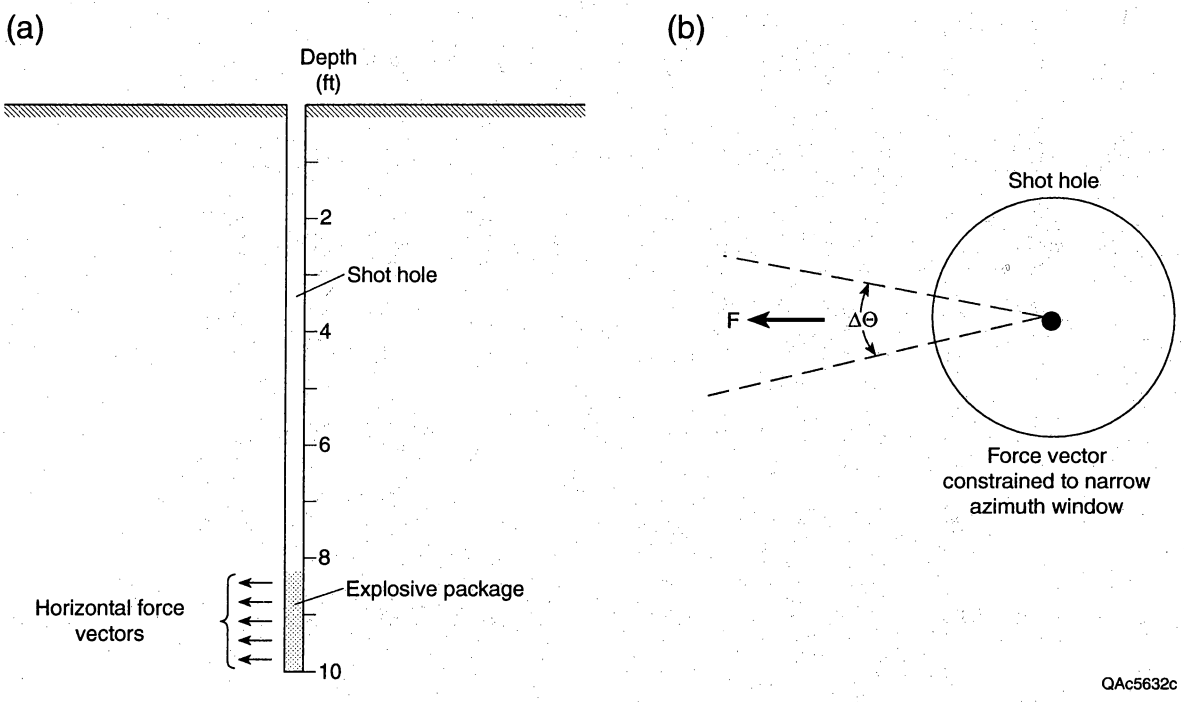

Fig. 3. An explosive package that generates S-waves. The packaging must (a) be easily deployed in standard shot holes and (b) generate a robust, horizontally directed force vector that is oriented in a narrow azimuth aperture $\Delta\theta$.

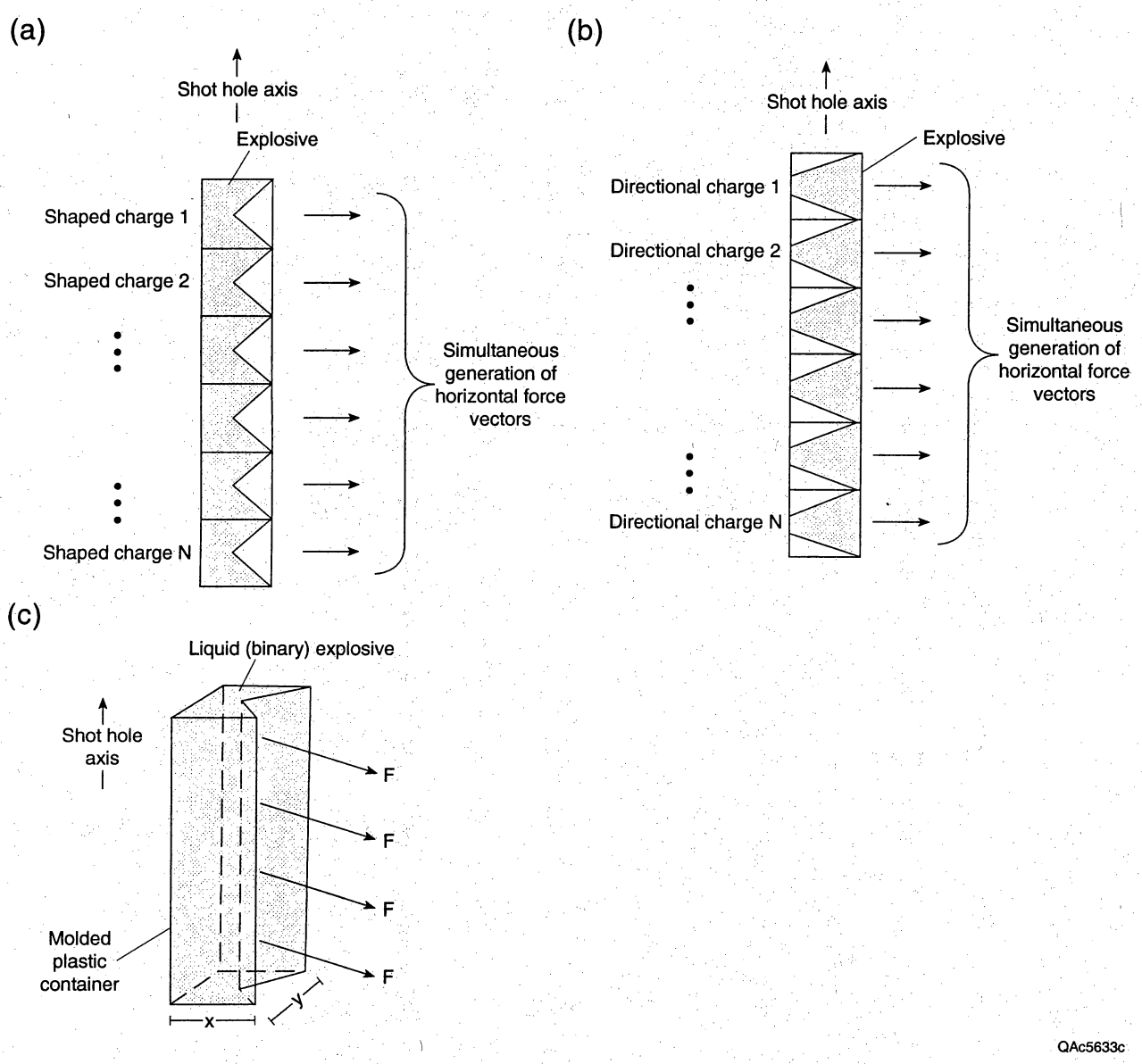

Fig. 4. (a) Shaped charge concept. The objective is to assemble shaped charges that have a length less than the diameter of a shot hole into a package that will allow all charges to be fired simultaneously to generate a horizontally oriented force vector. This illustration is a section view of such a package being detonated in a shot hole. (b) Directional charge concept. The charges must be horizontal in the hole and fire simultaneously to generate a robust, horizontally directed force vector. (c) Binary-liquid charge concept. The objective is to deploy a liquid binary-explosive in a plastic housing that is specially molded to create a horizontally directed, shaped-charge geometry in a small diameter shot hole. The lateral dimensions x and y of the plastic container must be small enough to allow the package to be inserted into standard shot holes. Force vectors F must be horizontal and focused in a narrow azimuth aperture.

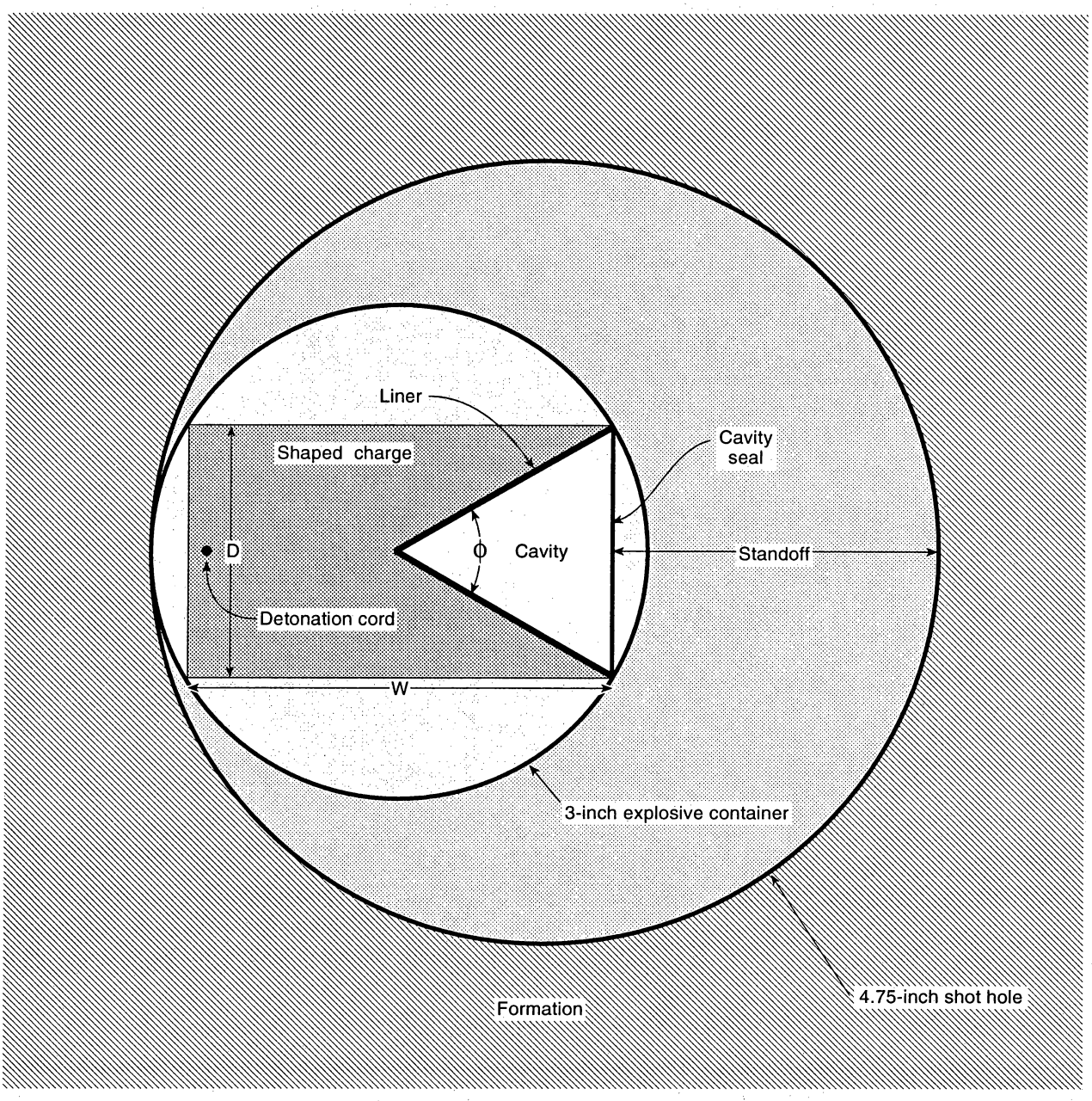

Fig. 5. Top view of a shaped-charge explosive package deployed in a shot hole. A 3-in diameter package and a 4.75-in shot hole are drawn to scale to show the relationship between charge size (D and W) and the maximum standoff distance.

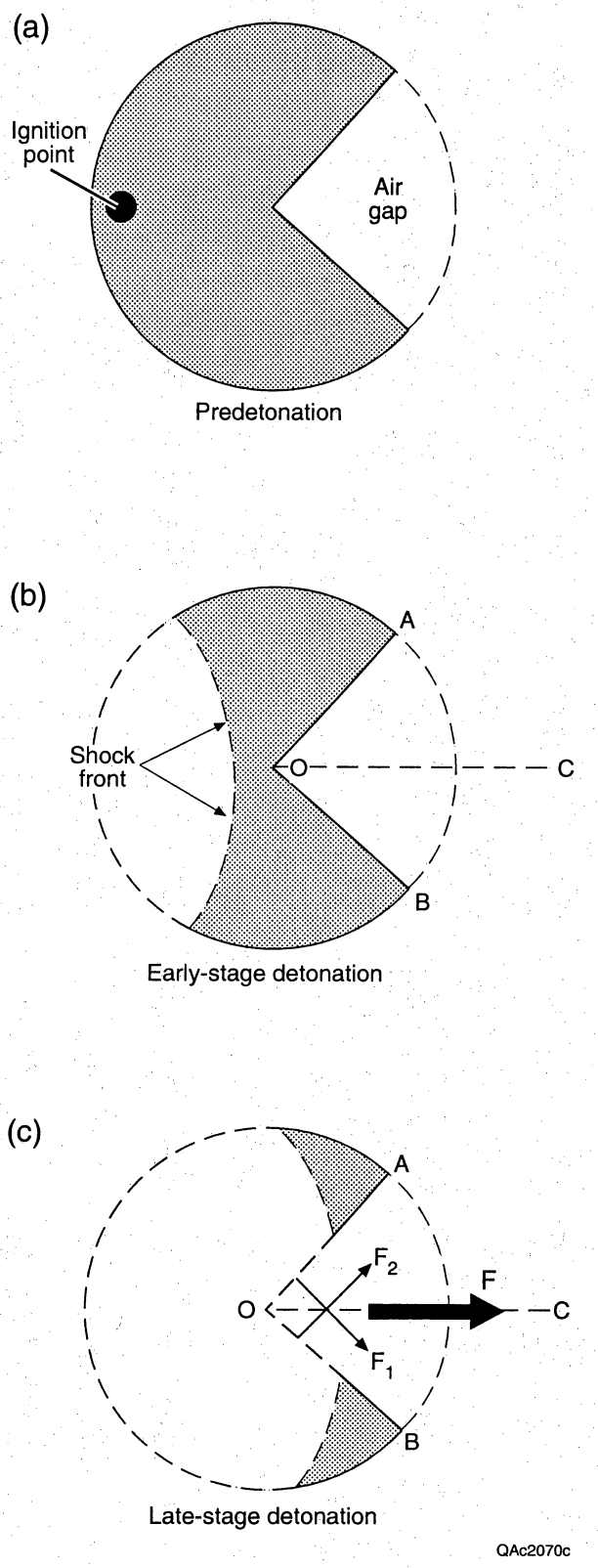

Fig. 6. Vertical view of shaped charge at various stages of detonation. (a) The detonation front is created at an ignition point that is directly opposite the shaped notch BOA. As the shock front sweeps past the notch (b and c), it creates counter-opposed forces F_1 and F_2 that sum as vectors to create a strong horizontal force **F**.

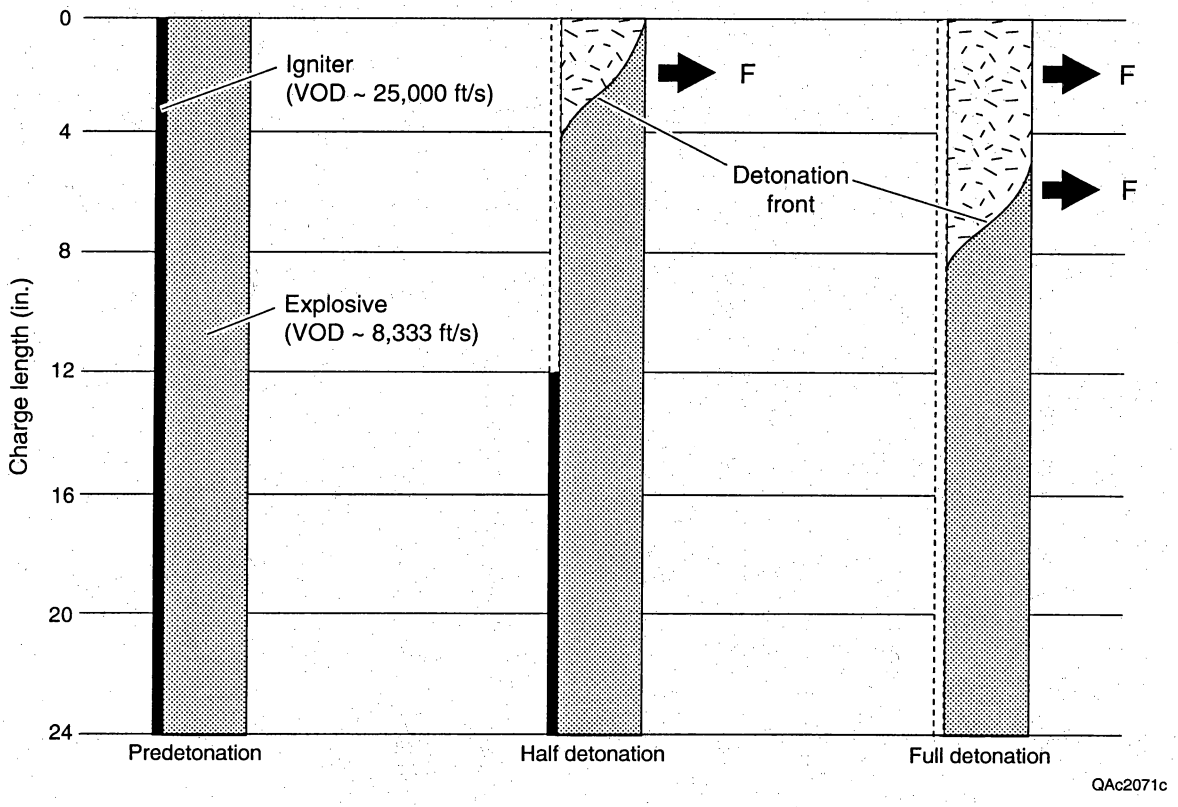

Fig. 7. Side view of shaped charge at various stages of detonation. A high-velocity igniter cord extends the full length of the charge (a). The VOD in this igniter cord is three times greater than the VOD in the explosive, causing the detonation front in the explosive to lag the detonation in the igniter cord as shown in (b) and (c). The force vector **F** is the same force vector shown in Figure 6.

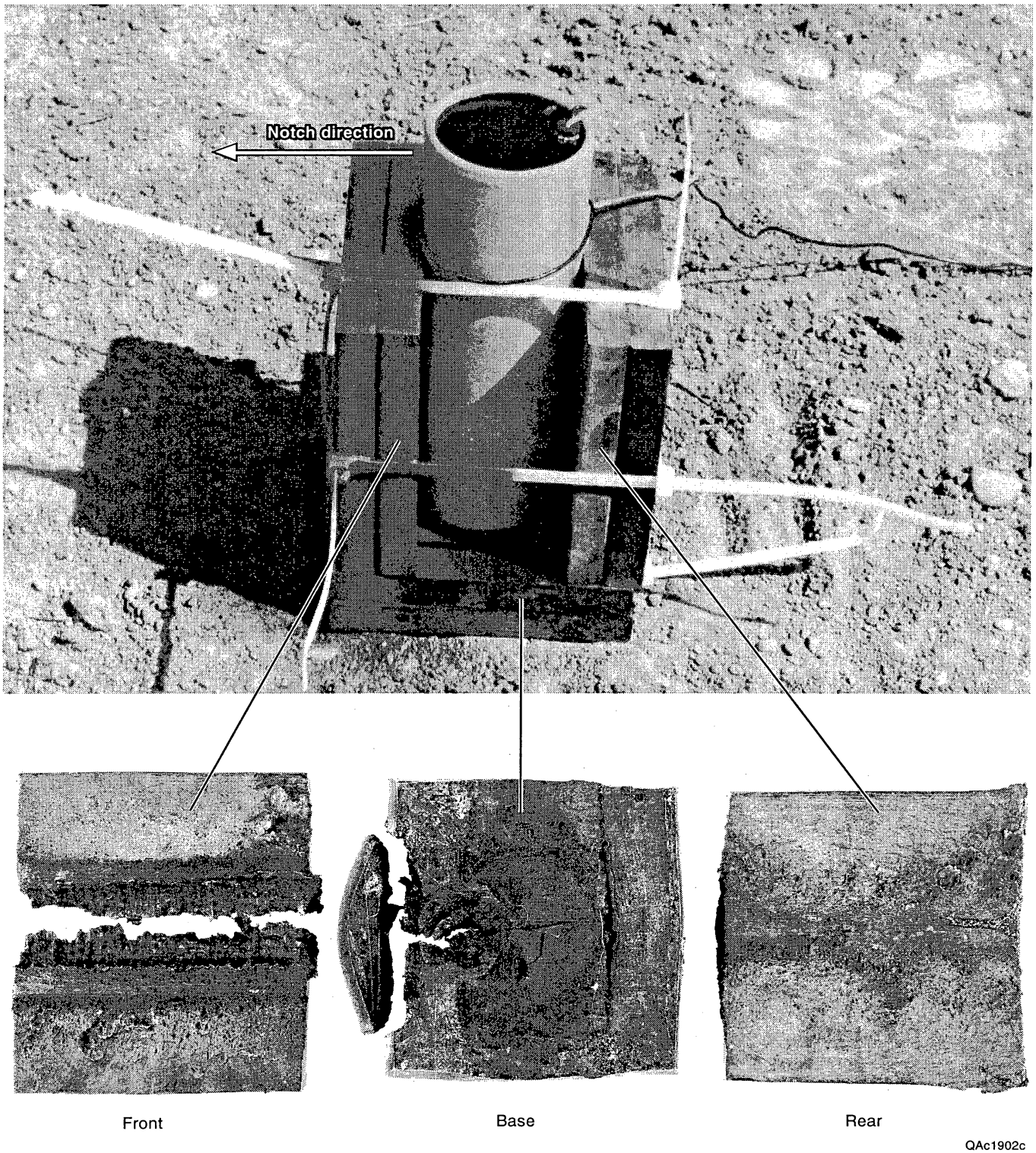

Fig. 8. Deformation test demonstrating the directional force produced by a pentolite shaped charge. The shaped charge is surrounded by two layers of 0.5-inch steel plates (top). The deformation of the inner layer of plates (bottom) shows that the greatest force is in the direction that the shaped-charge notch faces. When such a charge is oriented vertically in a shot hole, the detonation will create a horizontally directed force vector.

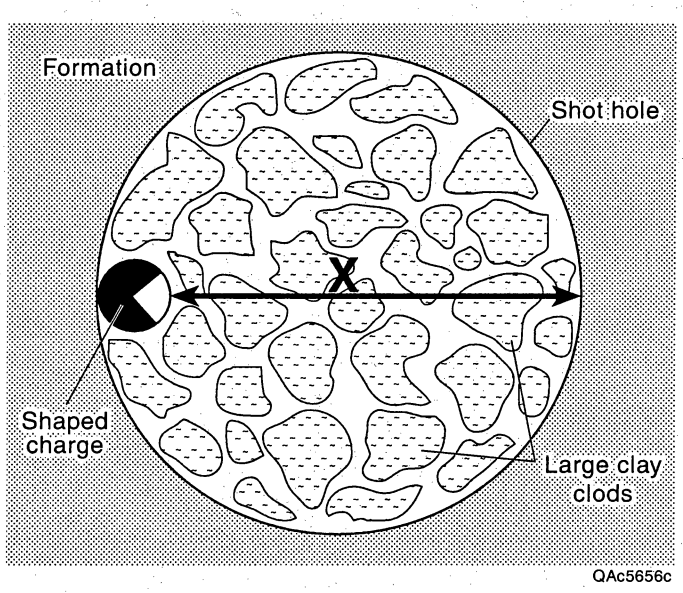

Fig. 9. Shot-hole conditions for test of pentolite shaped charge. The shot-hole diameter (10 in) and the charge diameter (1.5 in) are drawn to scale to show that an excessive standoff existed between the charge and competent earth material, resulting in an inefficient horizontal impulse being generated.

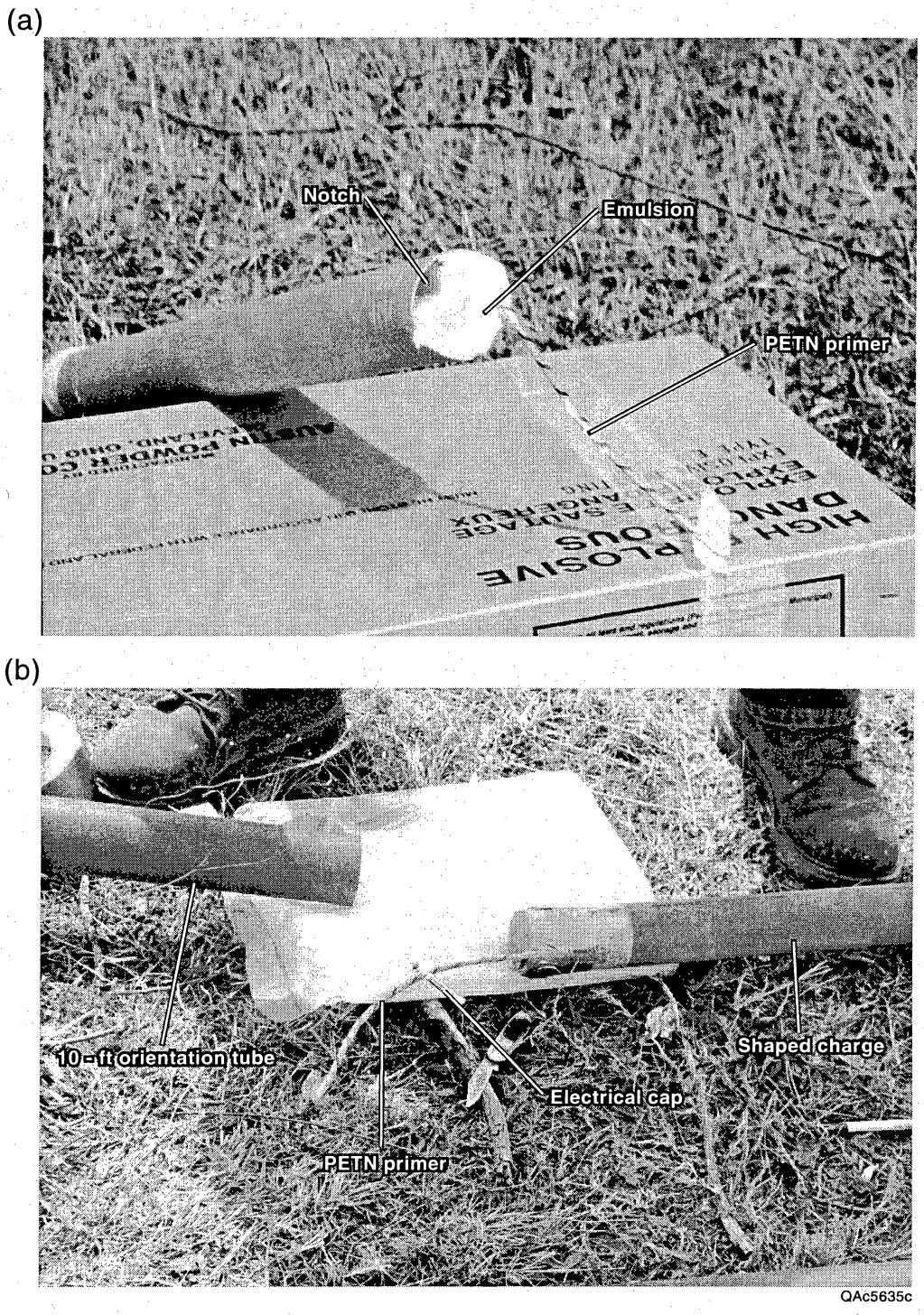

Fig. 10. (a) Low-velocity-emulsion shaped charge. (b) Package components ready for assembly.

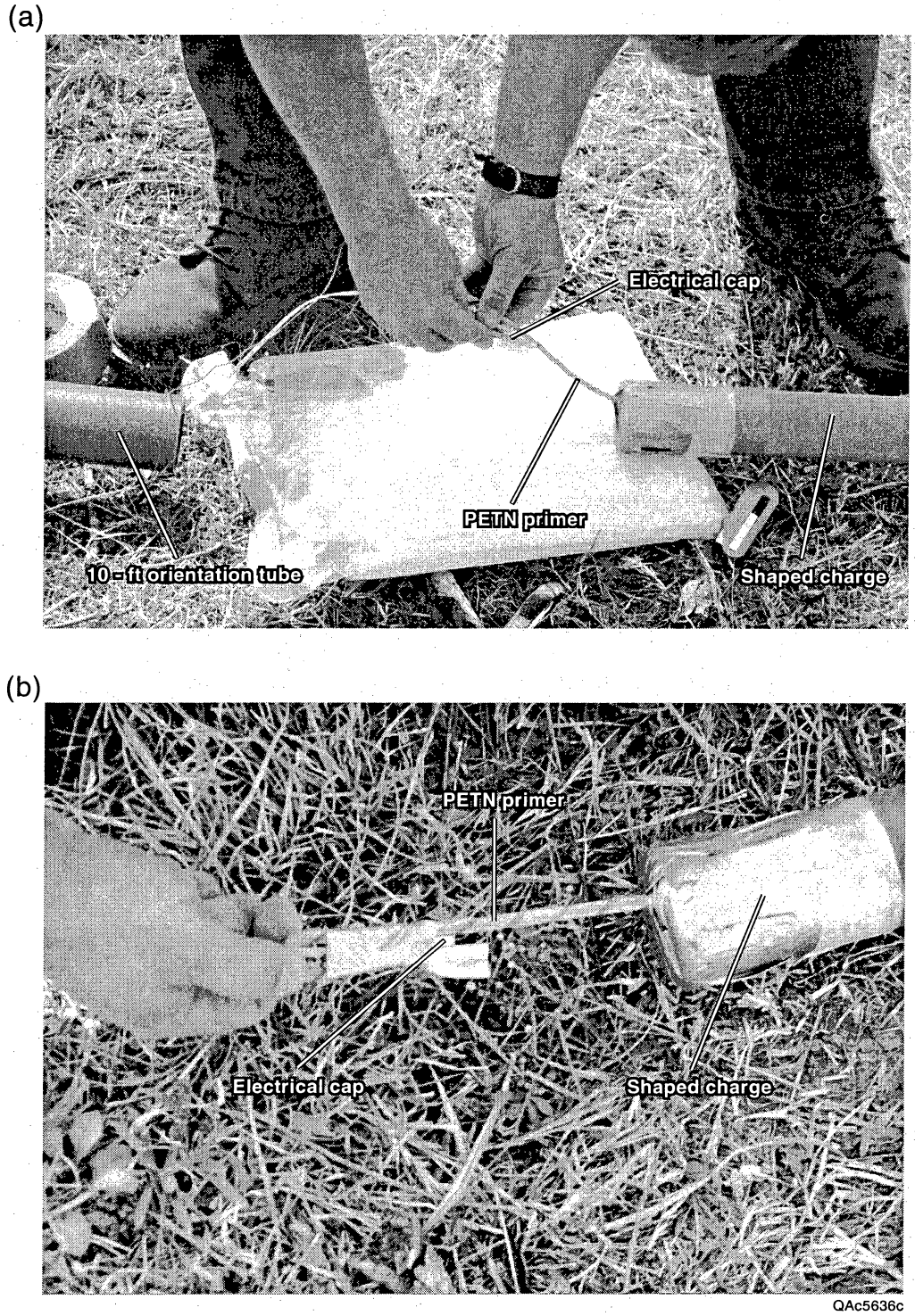

Fig. 11. (a) Low-velocity-emulsion shaped charge being prepared for detonation. (b) Proper union between cap and folded primer cord.

(a)

(b)

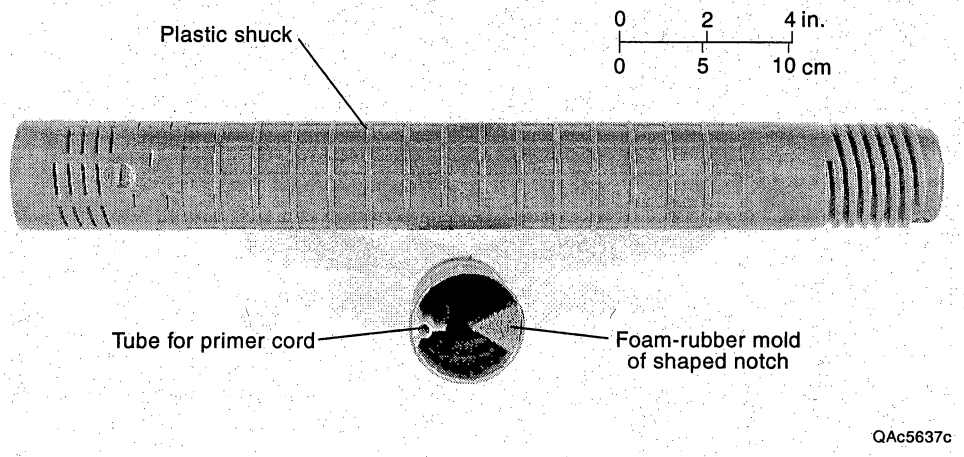

Fig. 12. (a) Full view of 10-ft orientation tube. Plastic tie strips are wrapped around the tube and tightened to bind the tube to the explosive package. A mark is then drawn on the outside of the tube to identify the location of the shaped notch. (b) The final design of the package for the low-velocity-emulsion explosive.

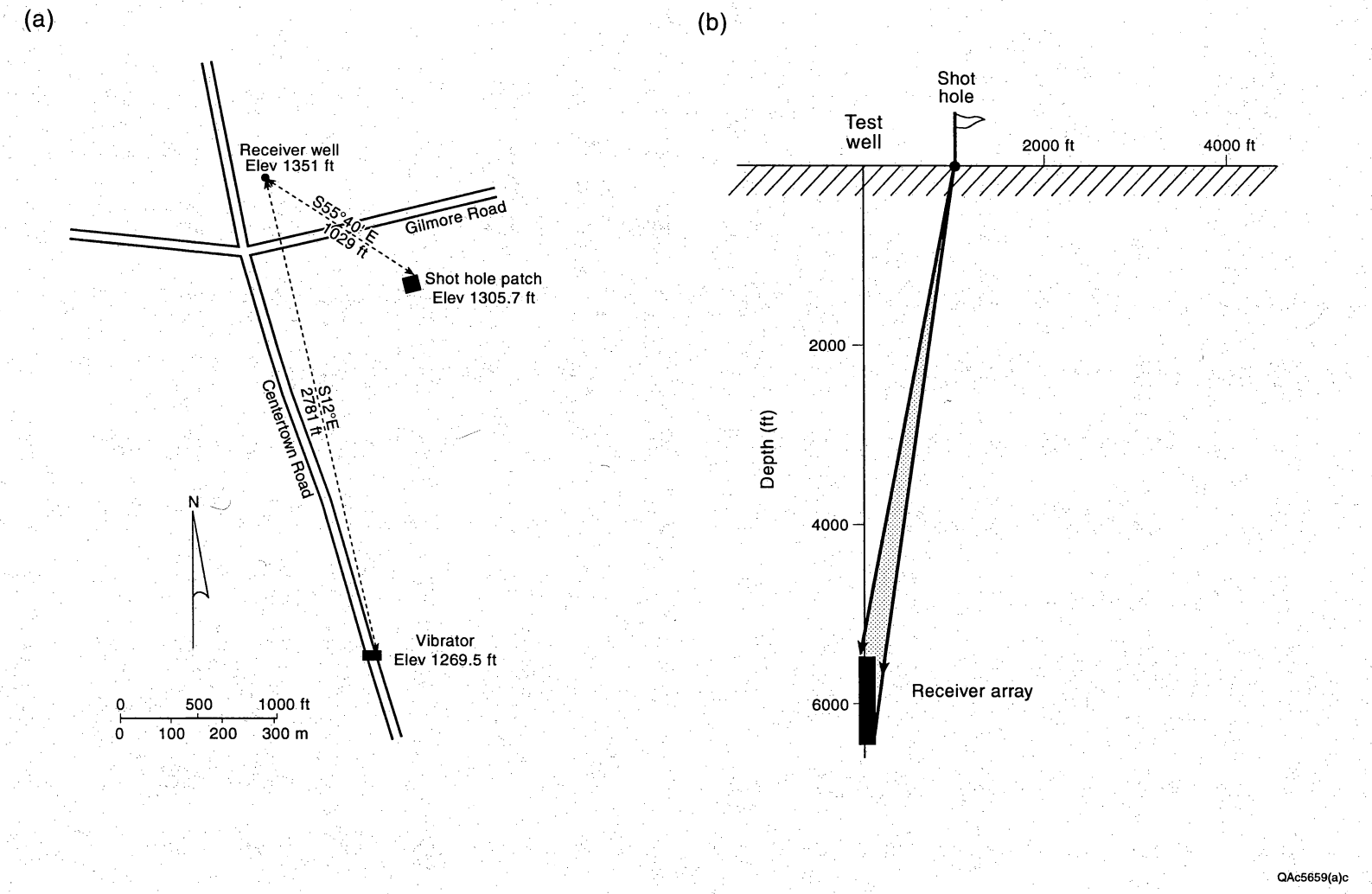

Fig. 13. Wavetest geometry used to evaluate low-velocity-emulsion shaped charge in Mercer County, Pennsylvania. (a) Downhole 3-C geophones were deployed in the receiver well; shaped charges were detonated in 10-ft shot holes inside the indicated shot-hole patch. Only one vibrator was at the south offset station to generate standard VSP data, not dipole-source data. (b) Section view drawn to scale to illustrate the near-vertical nature of the ray paths from the shot-hole patch to the restricted depth interval where geophone coupling could be achieved.

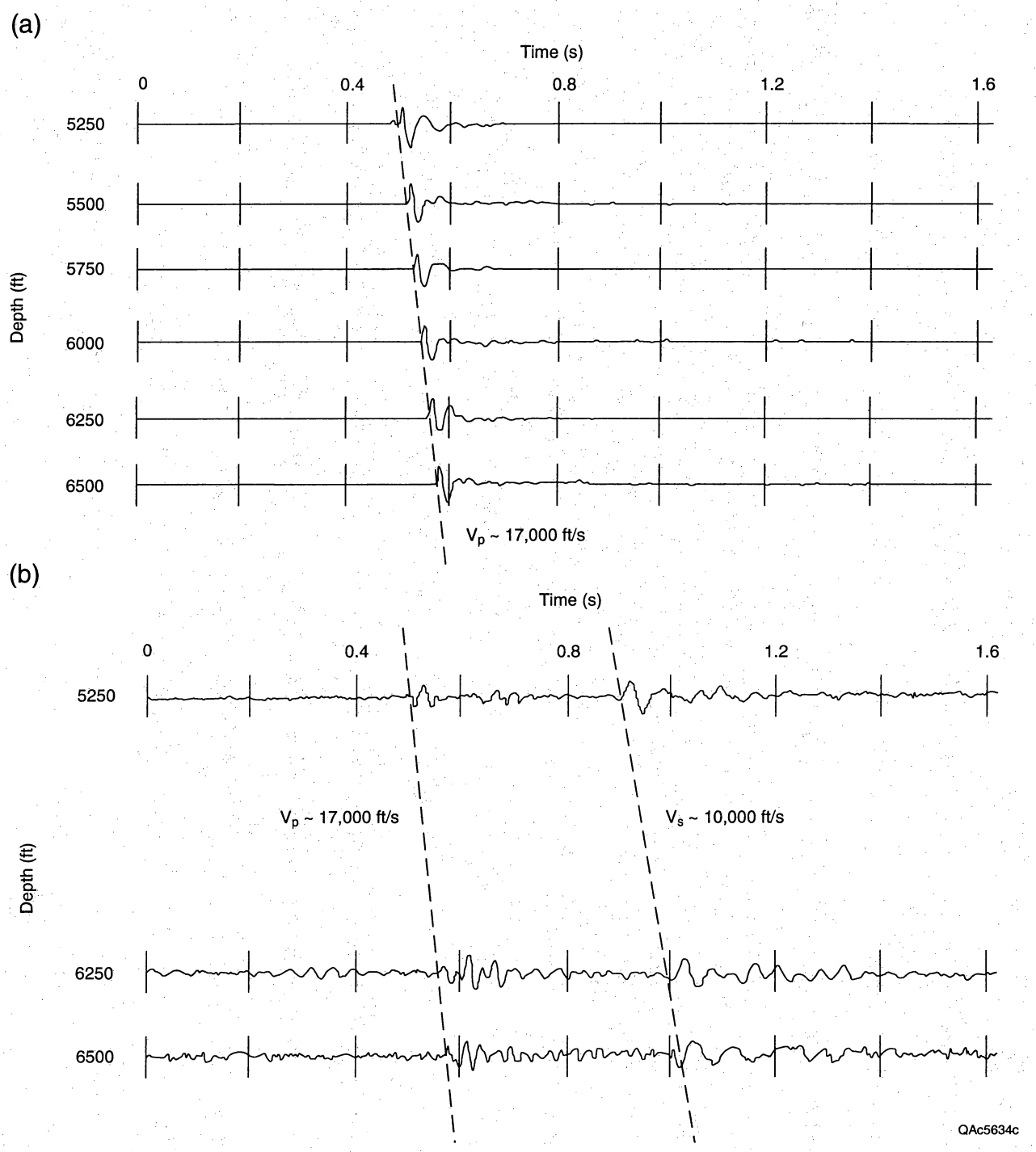

Fig. 14. (a) Wavefield recorded by vertically oriented downhole geophones. (b) Wavefield recorded by horizontally oriented downhole geophones. Traces are omitted at receiver stations where the horizontal receivers would not properly couple to the formation.

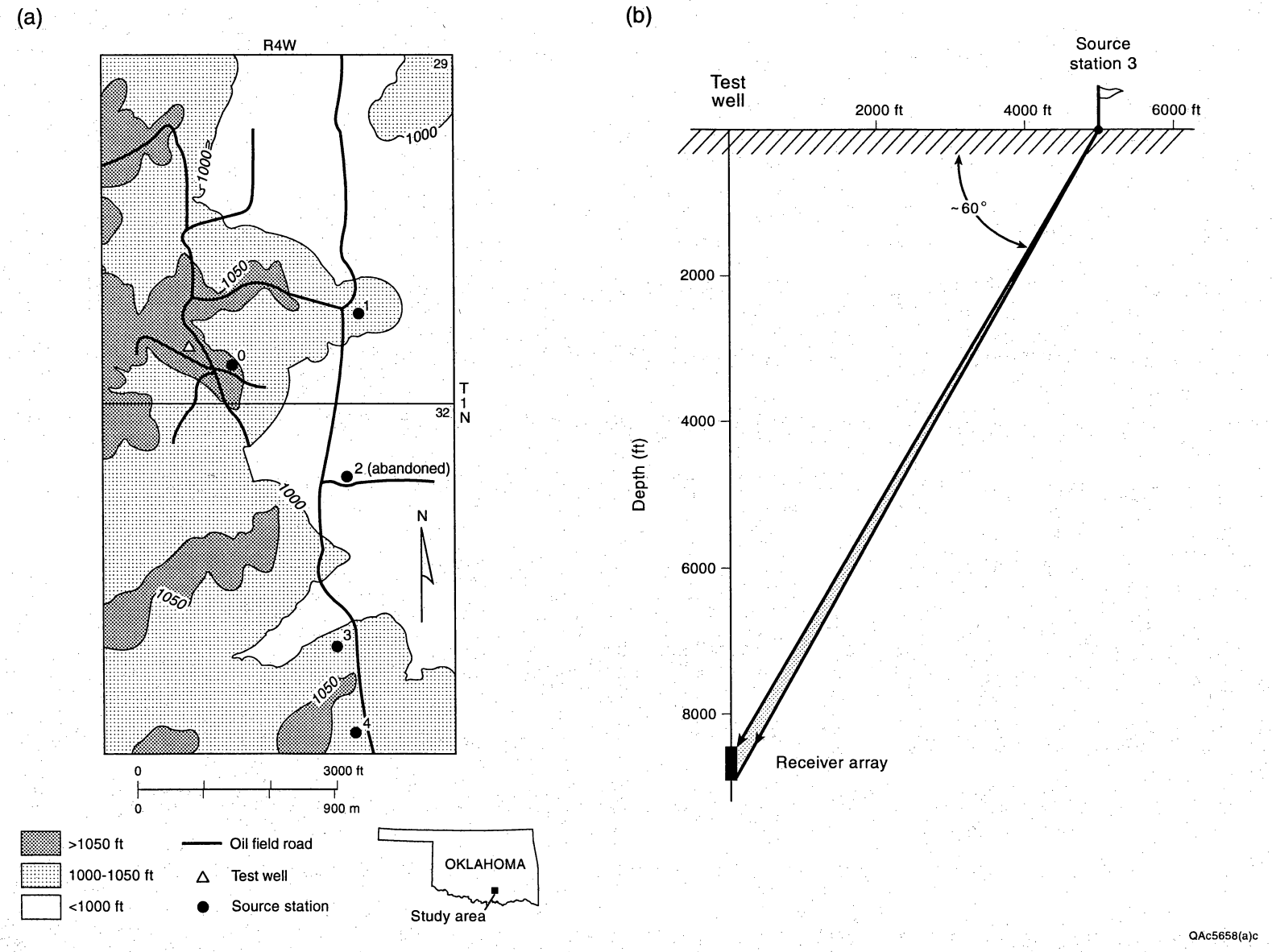

Fig. 15. Wavetest geometry used to evaluate low-velocity-emulsion charge in Stephens County, Oklahoma. (a) Map view. Test data were generated at station 3. (b) Section view showing raypath geometry.

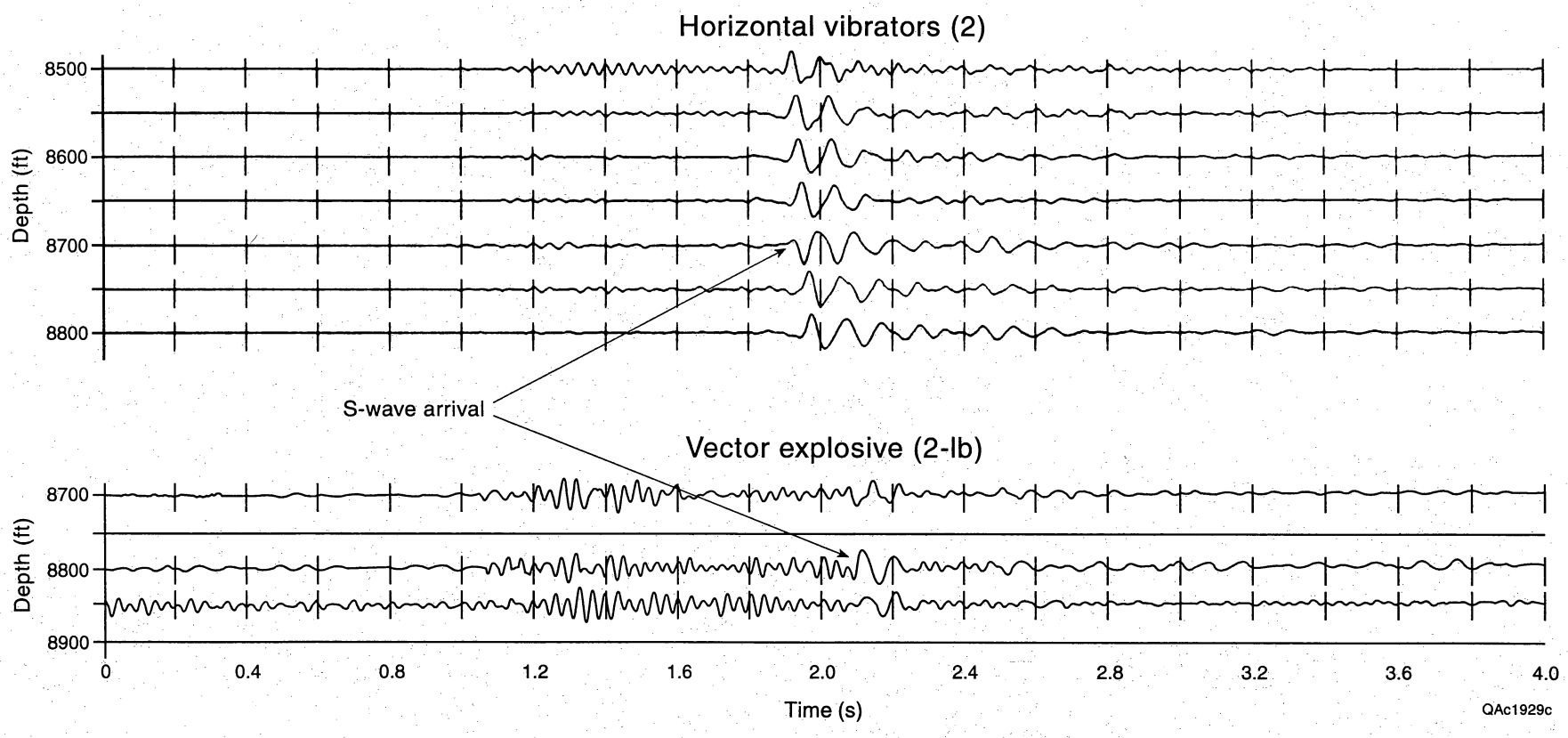

Fig. 16. Test data for (a) horizontal vibrator and (b) low-velocity-emulsion shaped charge. Data were recorded with horizontal geophones.

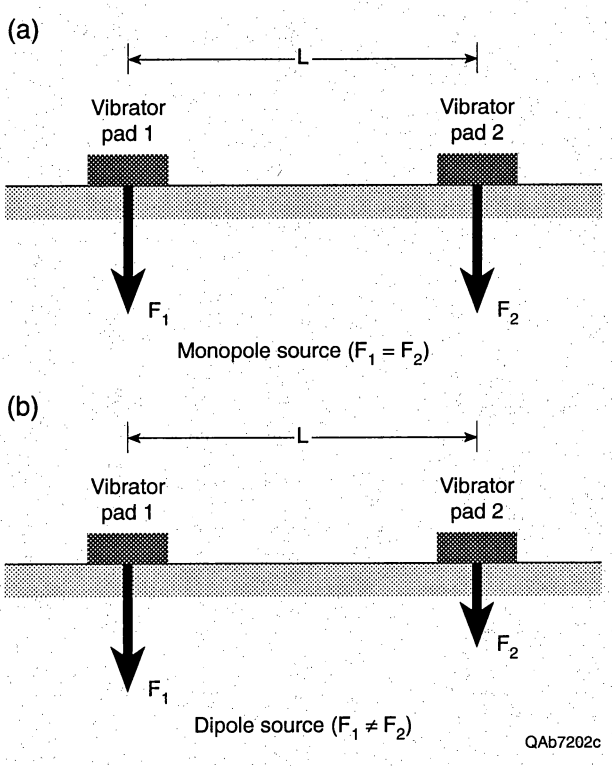

Fig. 17. A vertical-vibrator pair operating in monopole and dipole modes. (Top) If two vertical vibrator pads are a distance L apart and both vibrators generate identical ground-force vectors, the two-vibrator array forms a monopole source of dimension L. (Bottom) If the two vibrators generate force vectors with significantly different instantaneous magnitudes, they form a dipole source of length L.

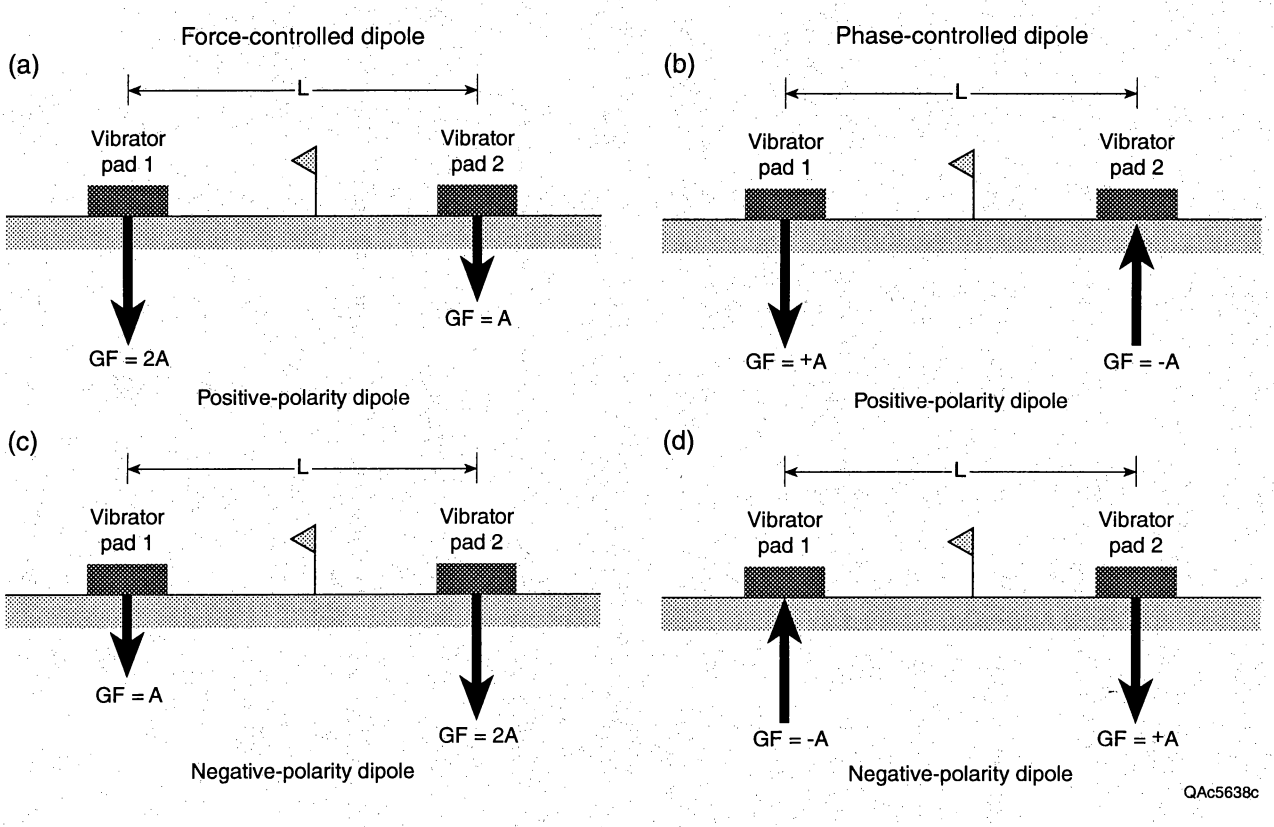

Fig. 18. (a and c) Principle of force-controlled dipole polarity. (b and d) Principle of phase-controlled dipole polarity. GF is the ground force created by the vibrator. The top dipoles are defined arbitrarily as having a positive polarity; the bottom dipoles have a negative polarity. The P-wave component of the wavefield emitted by each positive dipole is identical to the P-wave component of the wavefield created by the negative dipole. However, the polarity of the S-wave propagating away from the positive dipole should be opposite to the polarity of the S-wavefield propagating away from the negative dipole. A force imbalance of 2 is implied in a and c.

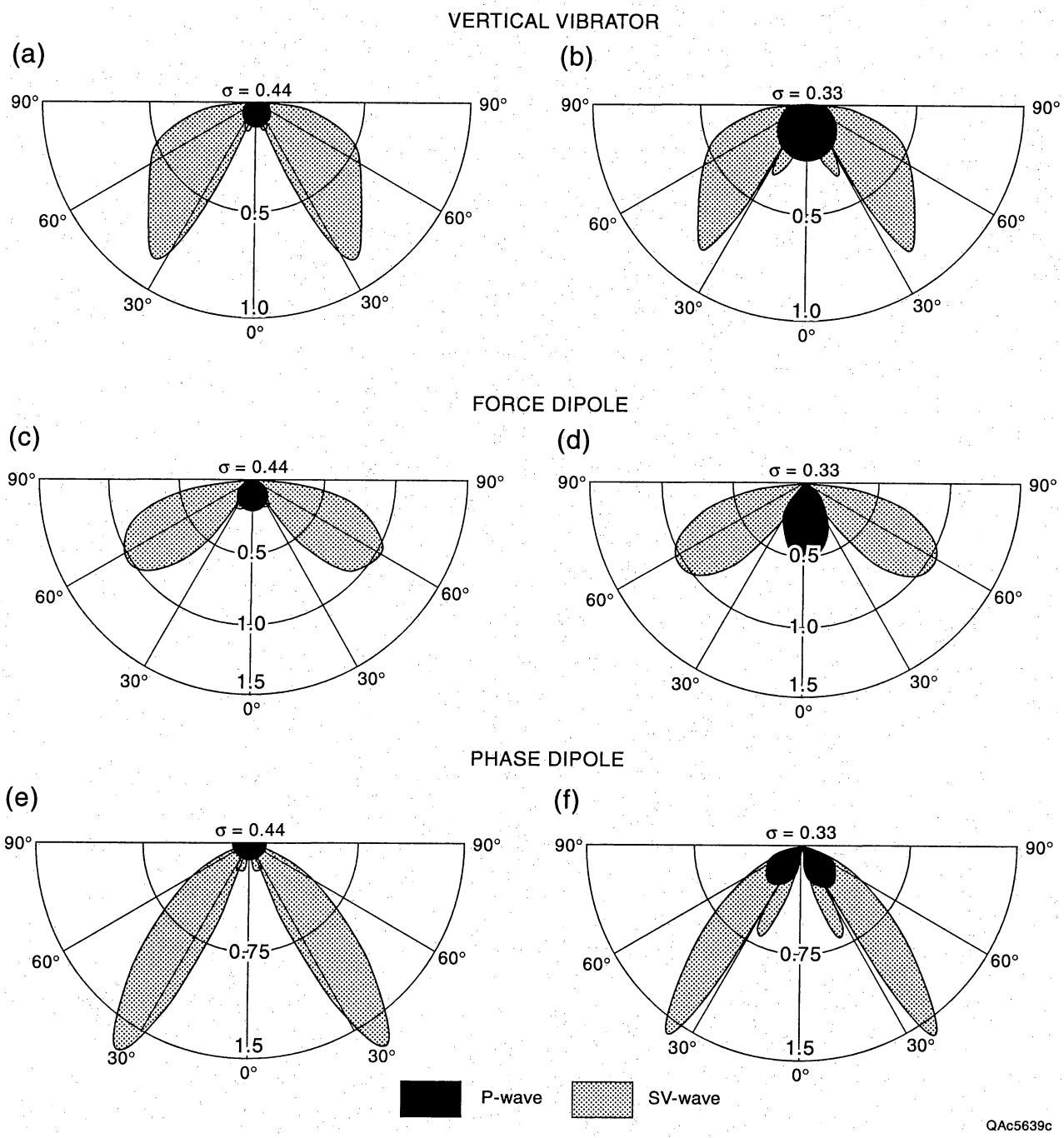

Fig. 19. Theoretical P and SV radiation patterns generated by a monopole (a, b), force dipole (c, d), and phase dipole (e, f). σ is Poisson's ratio. A force imbalance of 2 is implied in c and d.

(a)

QAc5643c

(b)

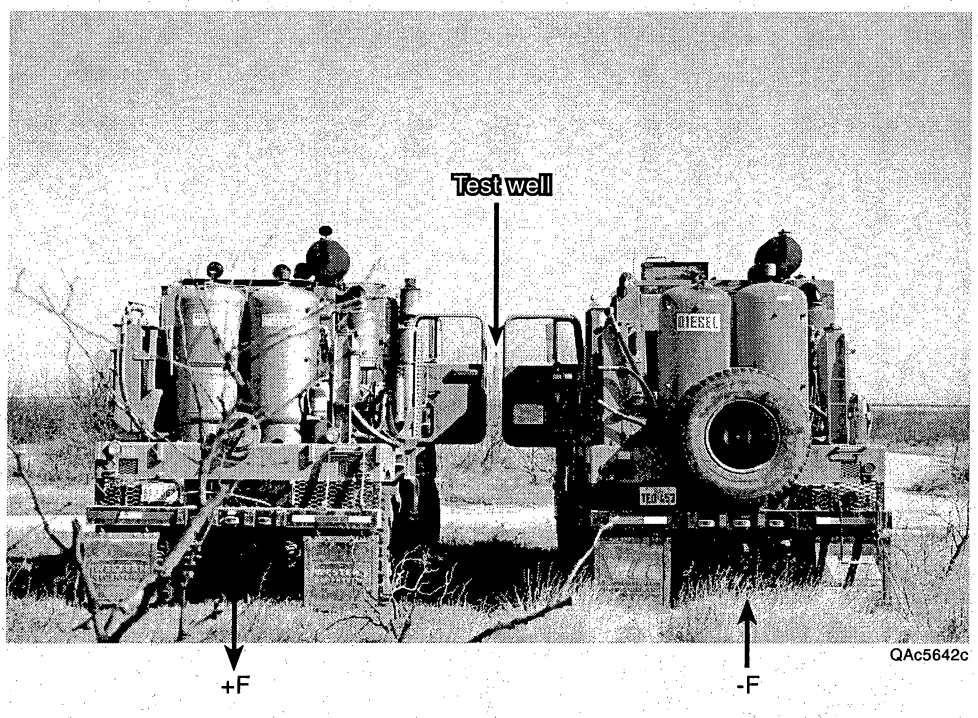

QAc5642c

QAc5642(a)c

Fig. 20. Photographs of vertical vibrators operating as a force dipole with a force imbalance of 2 (a) and as a phase dipole with a phase imbalance of 180° (b). Vibrator pads are 12 ft apart.

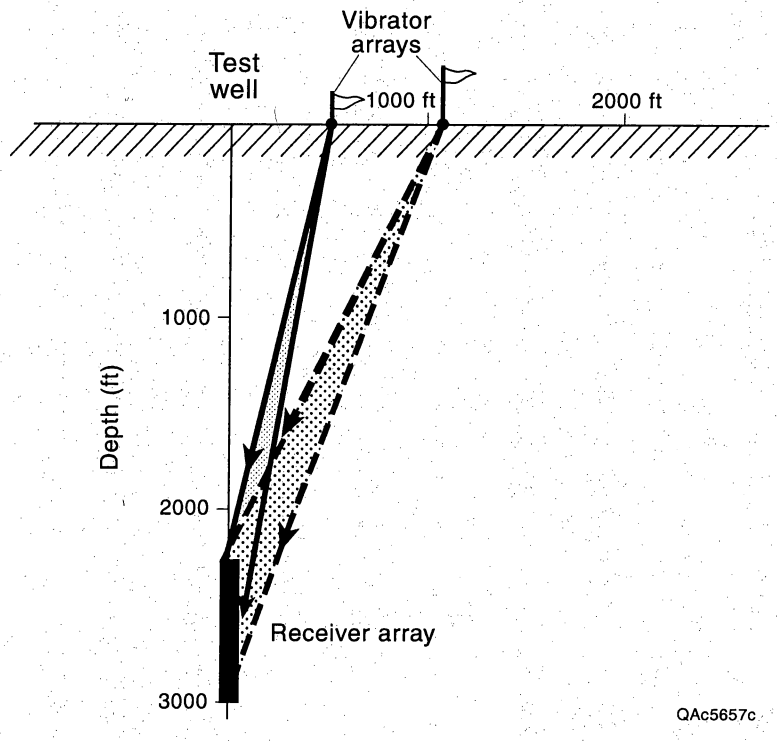

Fig. 21. Vertical wavetest geometry, Glacier County, Montana. The downhole vertical receiver array extends from 2950 to 2300 ft.

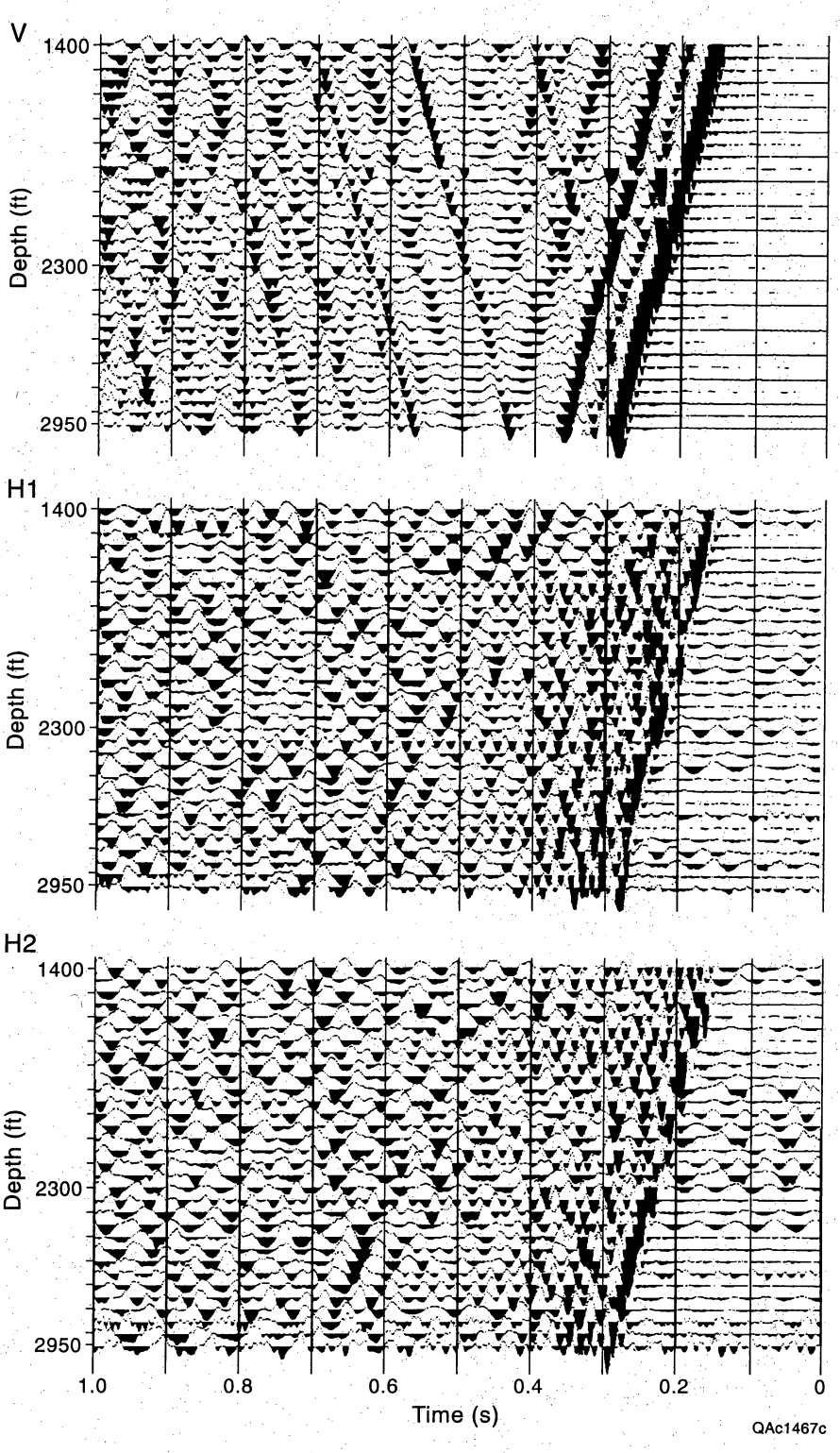

Fig. 22. Monopole data, 550-ft offset. V is the vertical geophone; H1 and H2 are horizontal geophones.

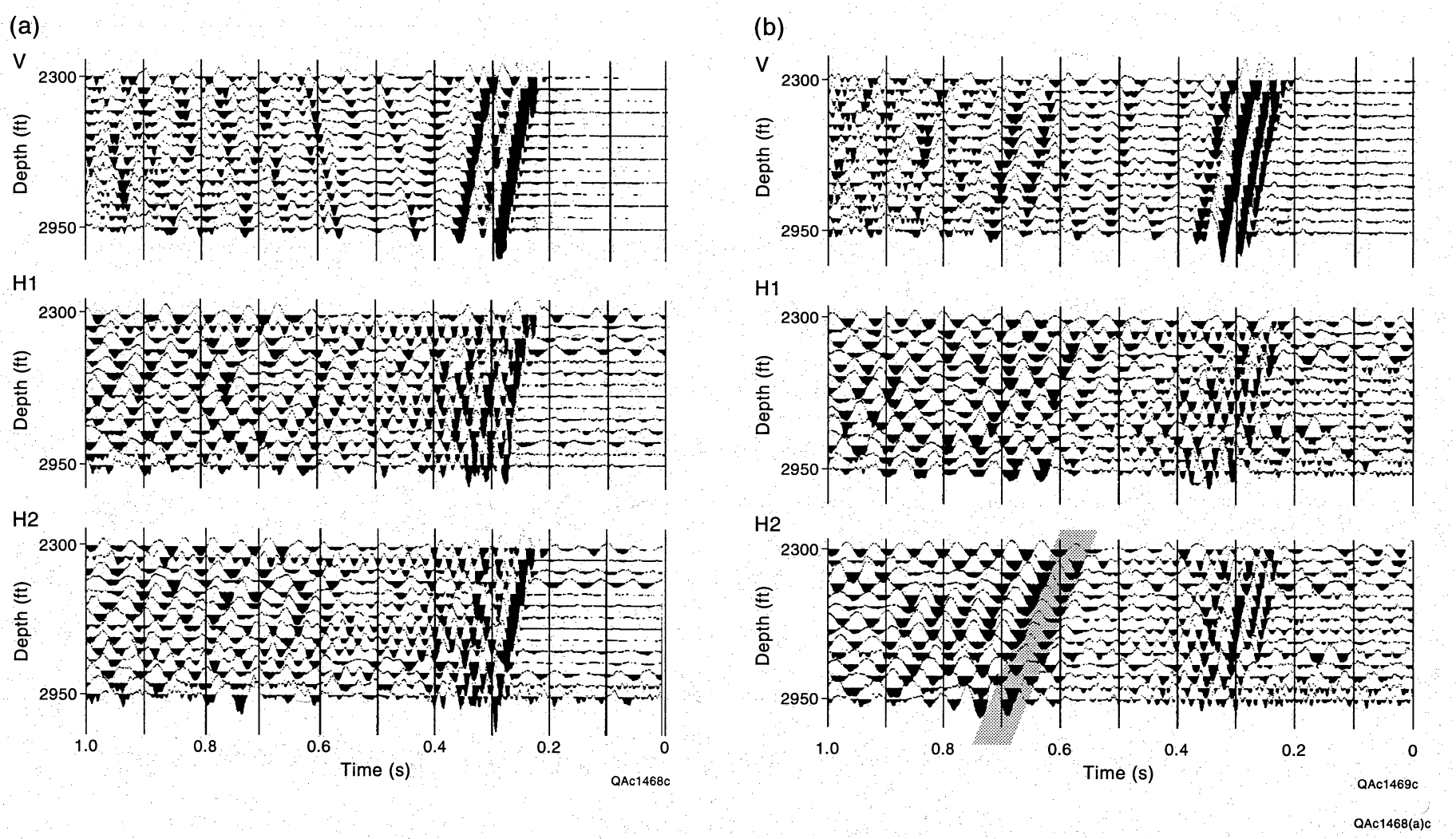

Fig. 23. Force-dipole (a) and phase-dipole (b) data, 550-ft offset. The shaded window (b, H2) highlights a high-amplitude portion of the SV arrival. V is the vertical geophone; H1 and H2 are horizontal geophones.

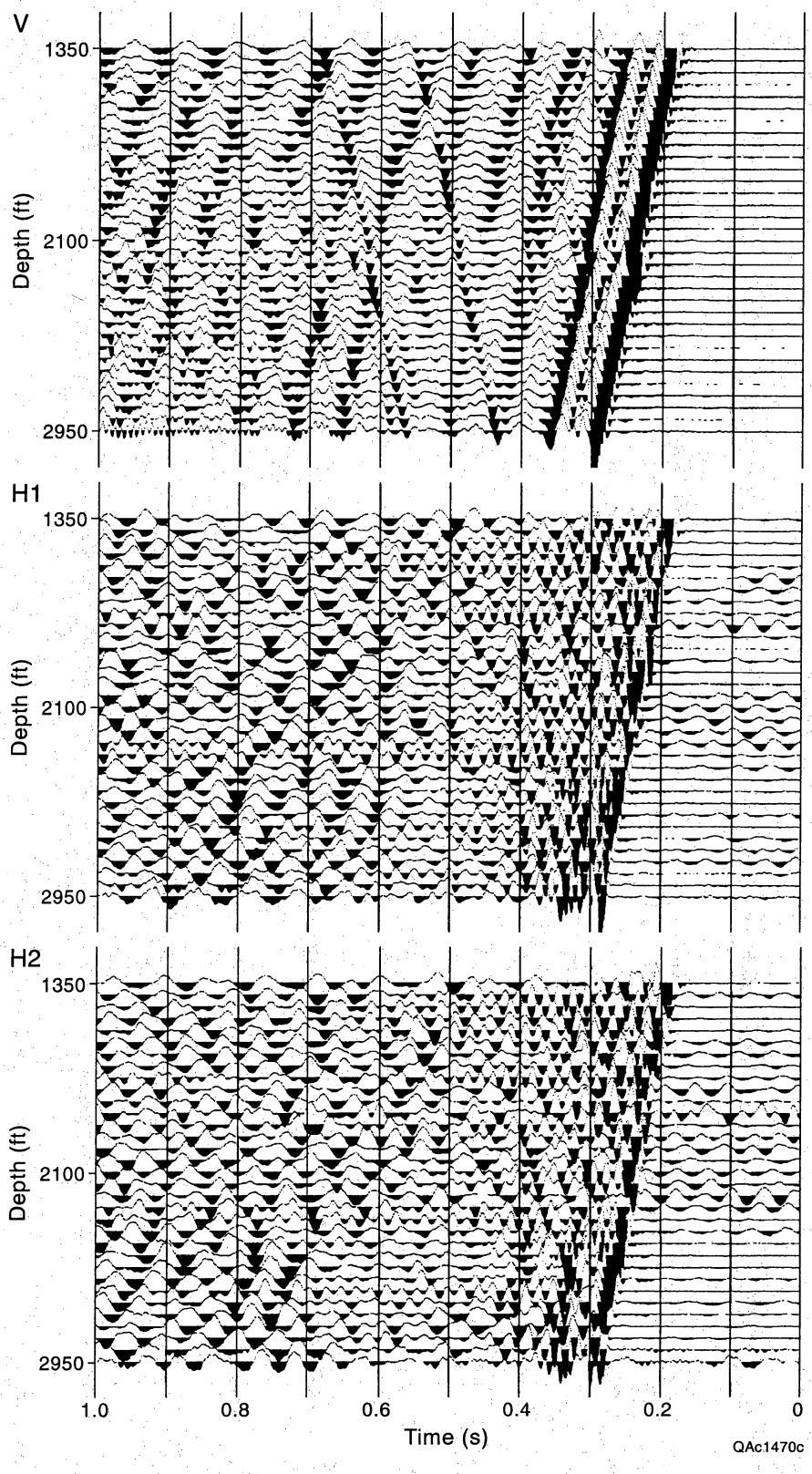

Fig. 24. Monopole data, 1,100-ft offset. V is the vertical geophone; H1 and H2 are horizontal geophones.

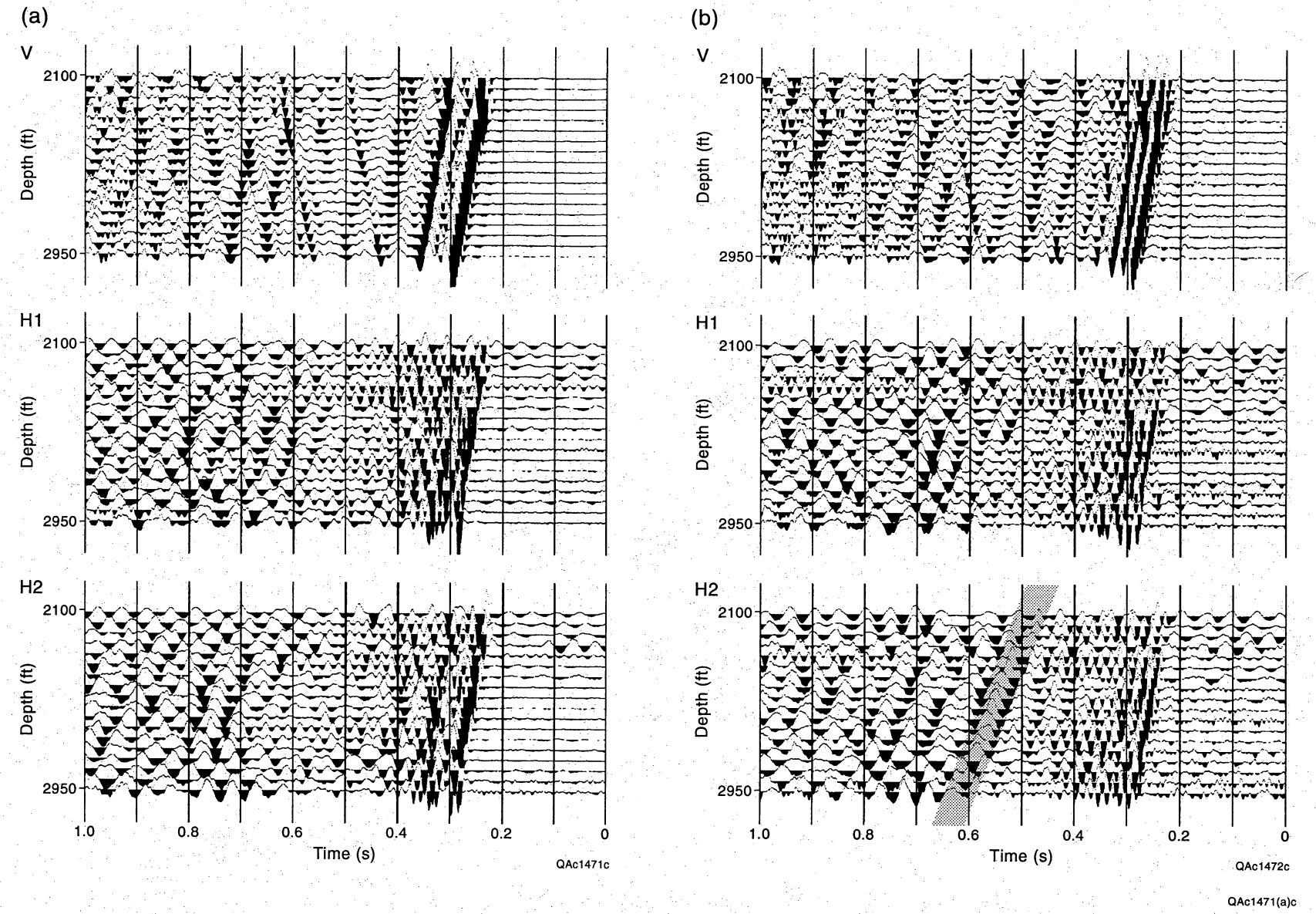

Fig. 25. Force-dipole (a) and phase-dipole (b) data, 1,100-ft offset. The shaded window (b, H2) highlights the SV arrival. V is the vertical geophone; H1 and H2 are horizontal geophones.

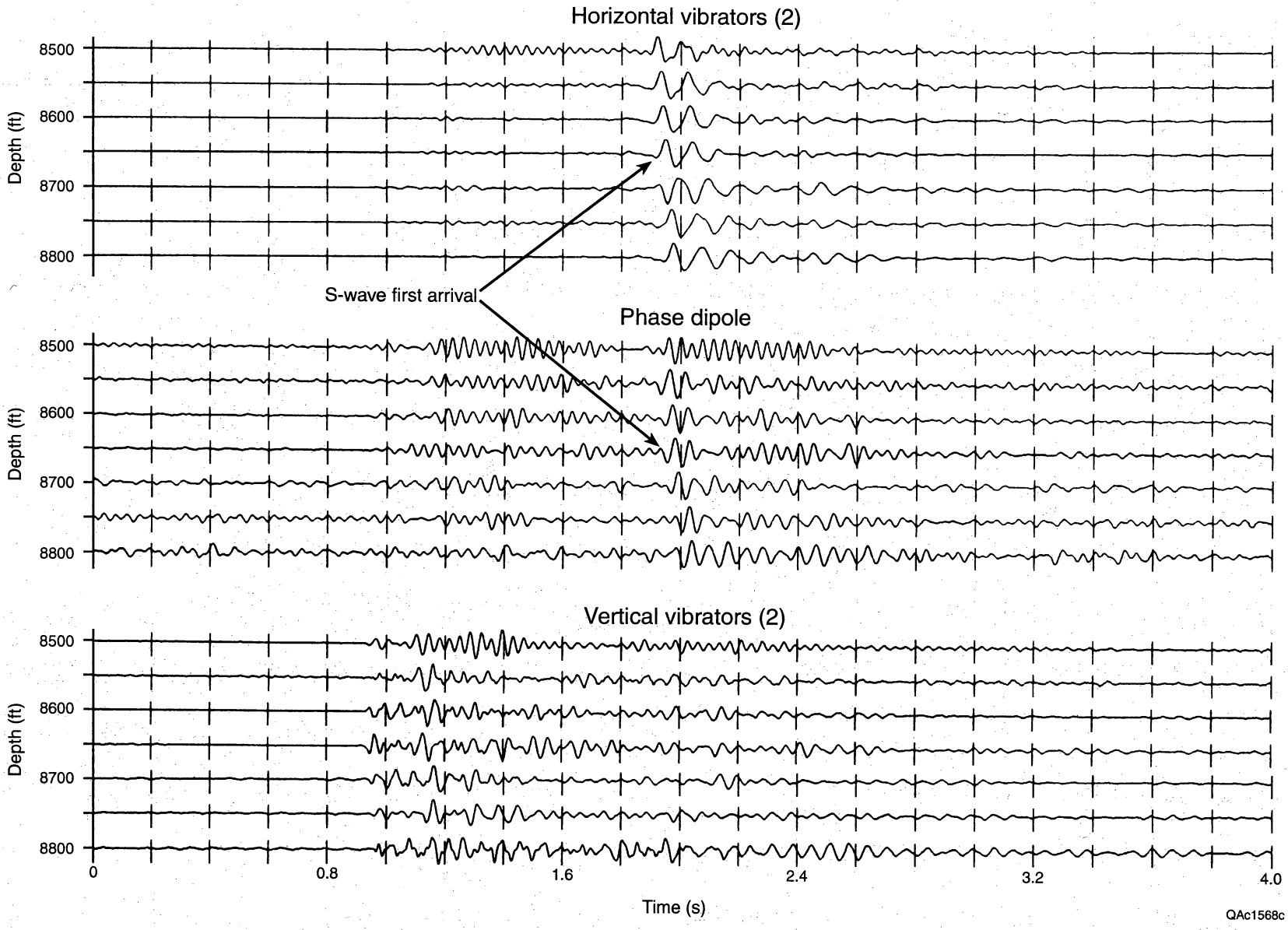

Fig. 26. Vertical wavetest data comparing downgoing S-wave first arrivals generated by horizontal vibrators (top), phase dipole (center), and a 2-element monopole of vertical vibrators (bottom). Data are recorded by downhole horizontal geophones. No S-wave event is present in the vertical-vibrator wavefield.

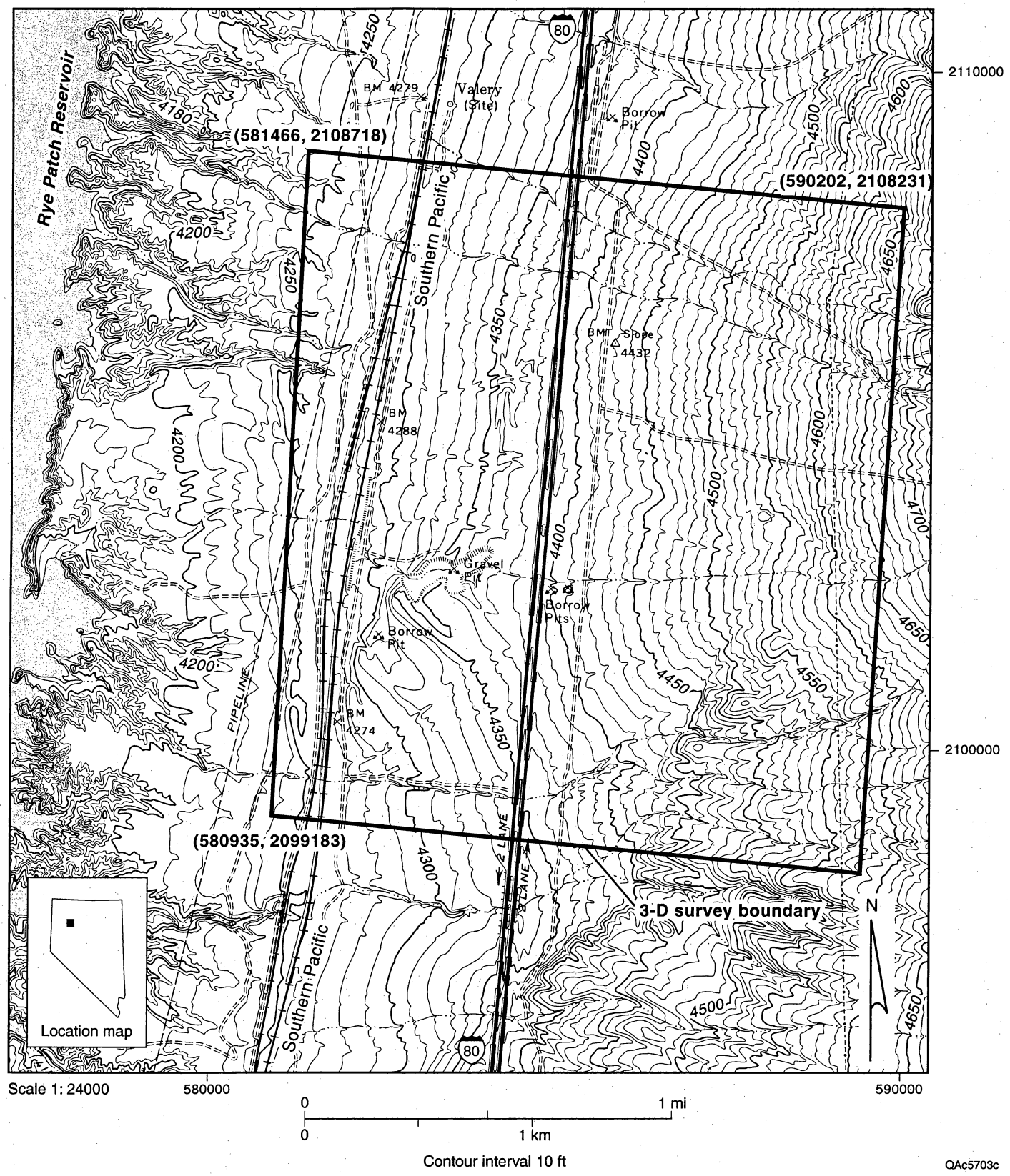

Fig. 27. Location of Rye Patch 3-D seismic survey.

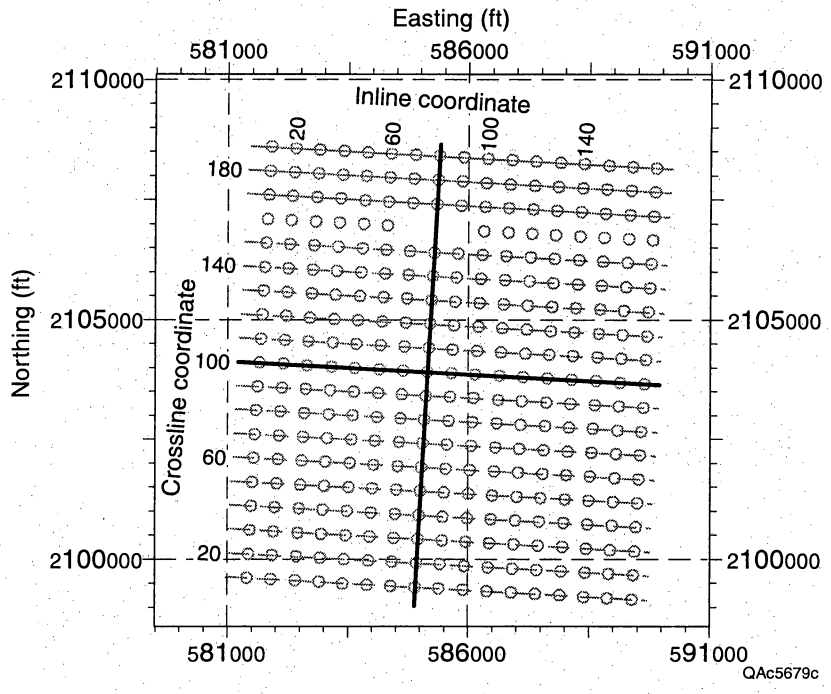

Fig. 28. Map specifying inline and crossline coordinates within the Rye Patch 3-D image space.

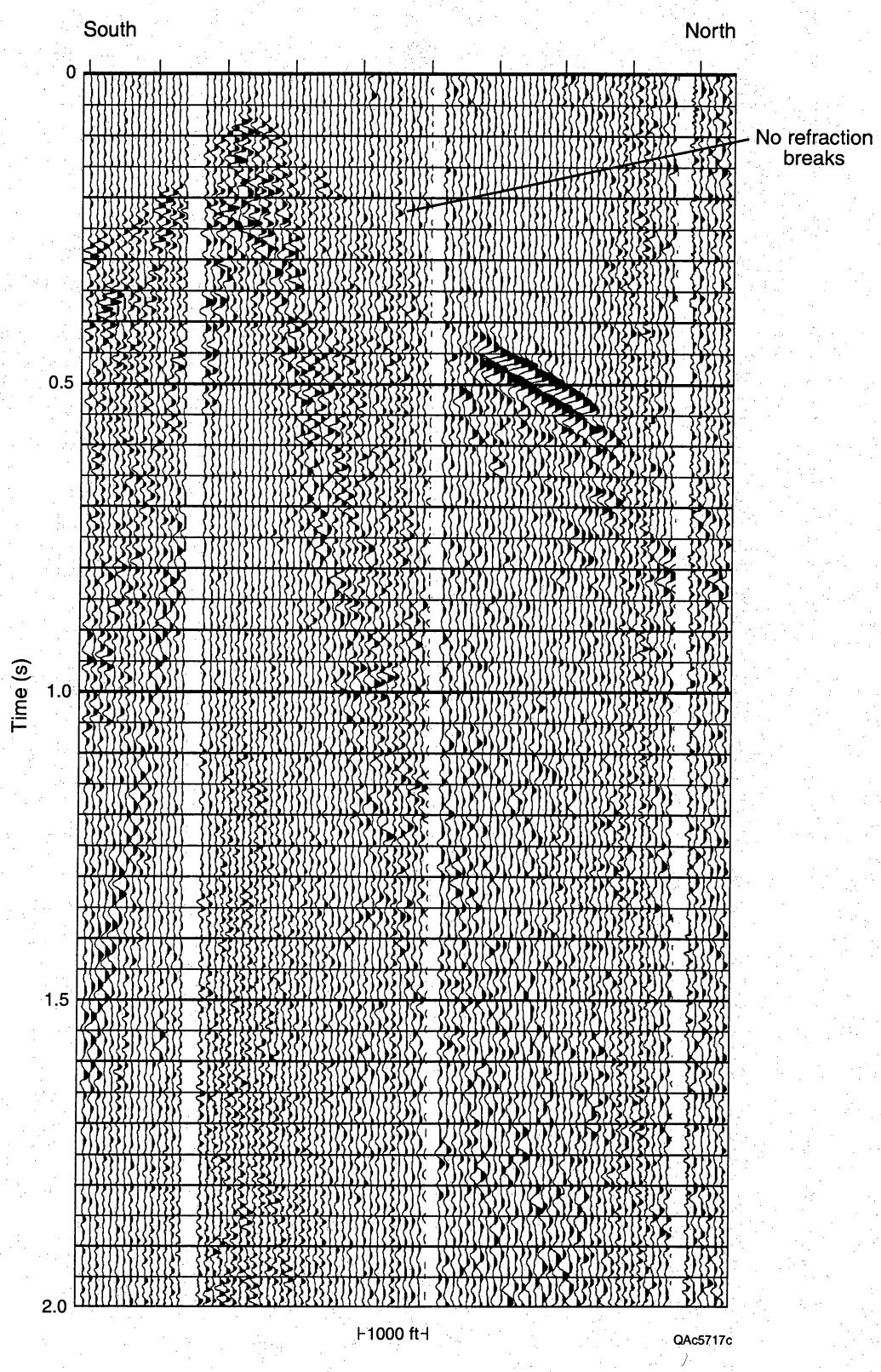

Fig. 29a. Example of field data recorded over Rye Patch field.

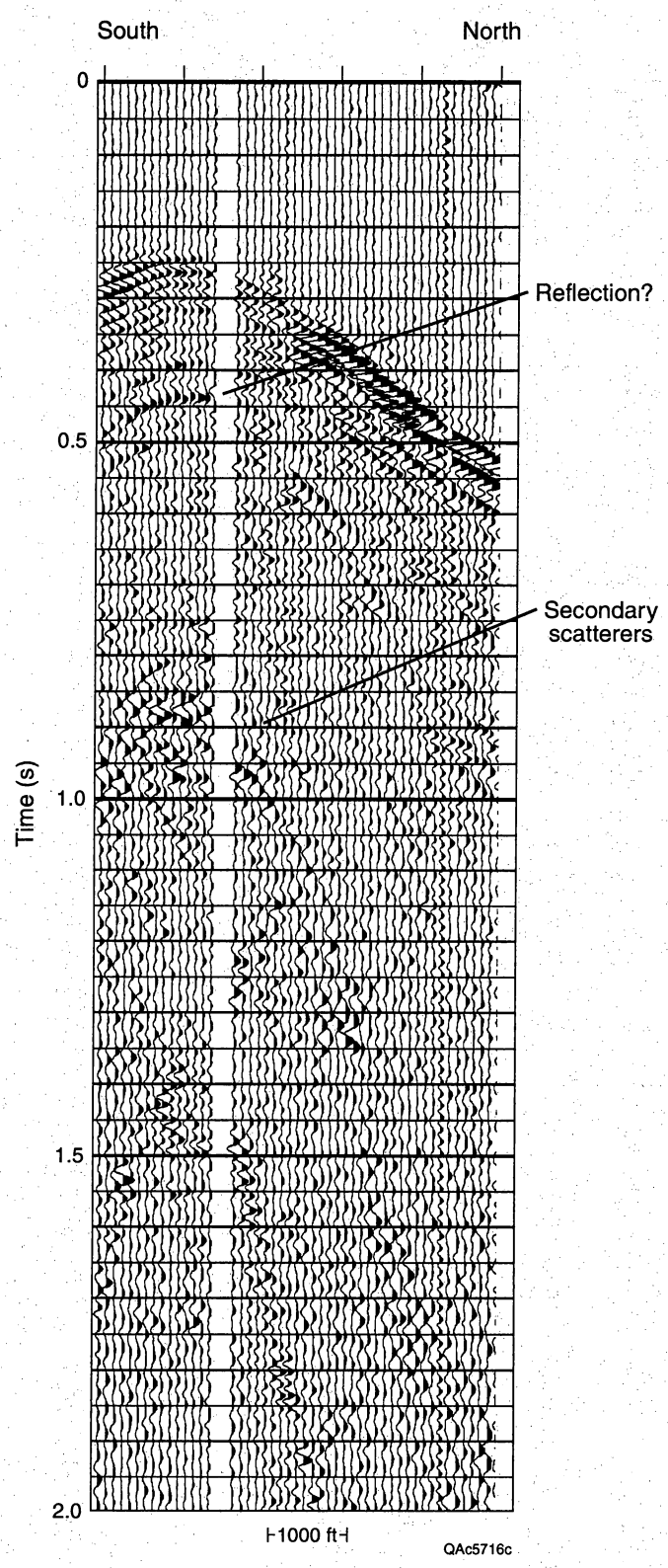

Fig. 29b. Example of field data recorded over Rye Patch field.

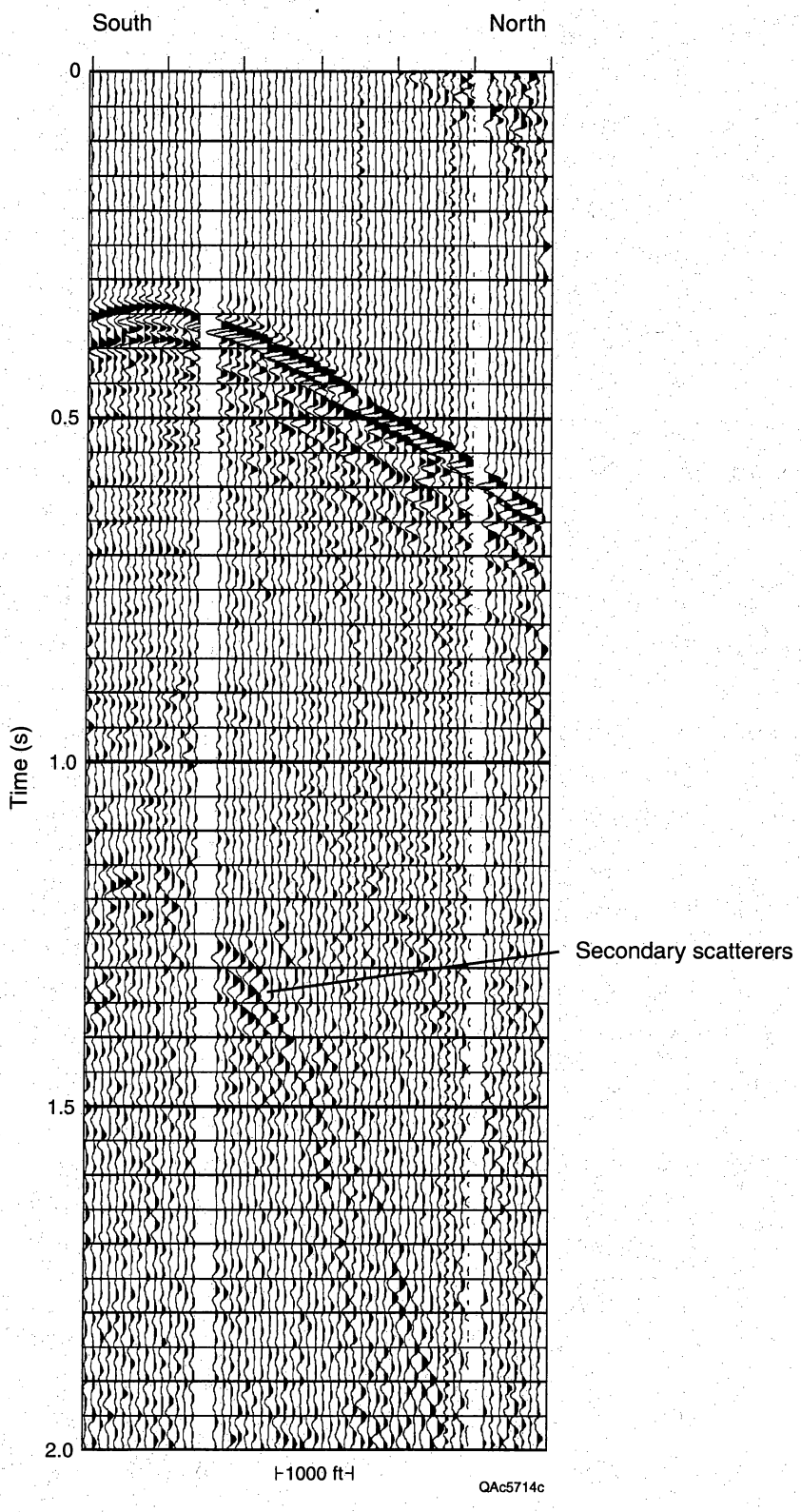

Fig. 29c. Example of field data recorded over Rye Patch field.

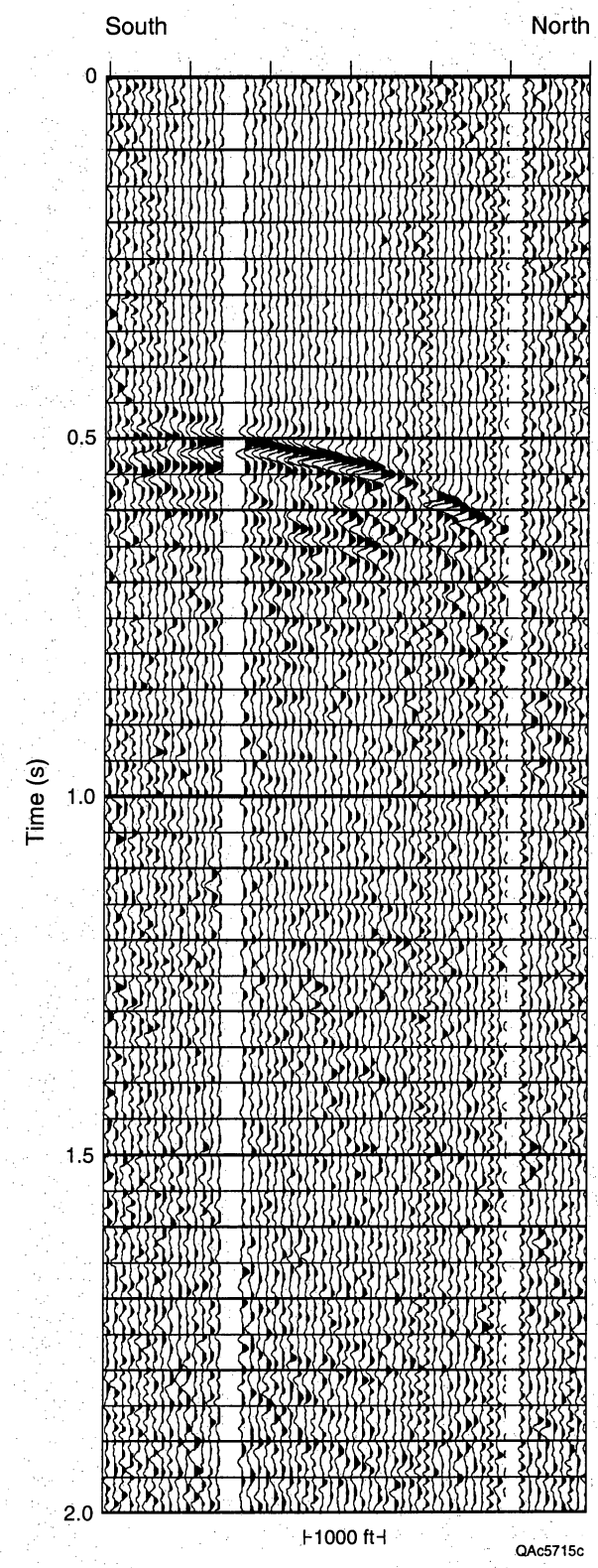

Fig. 29d. Example of field data recorded over Rye Patch field.

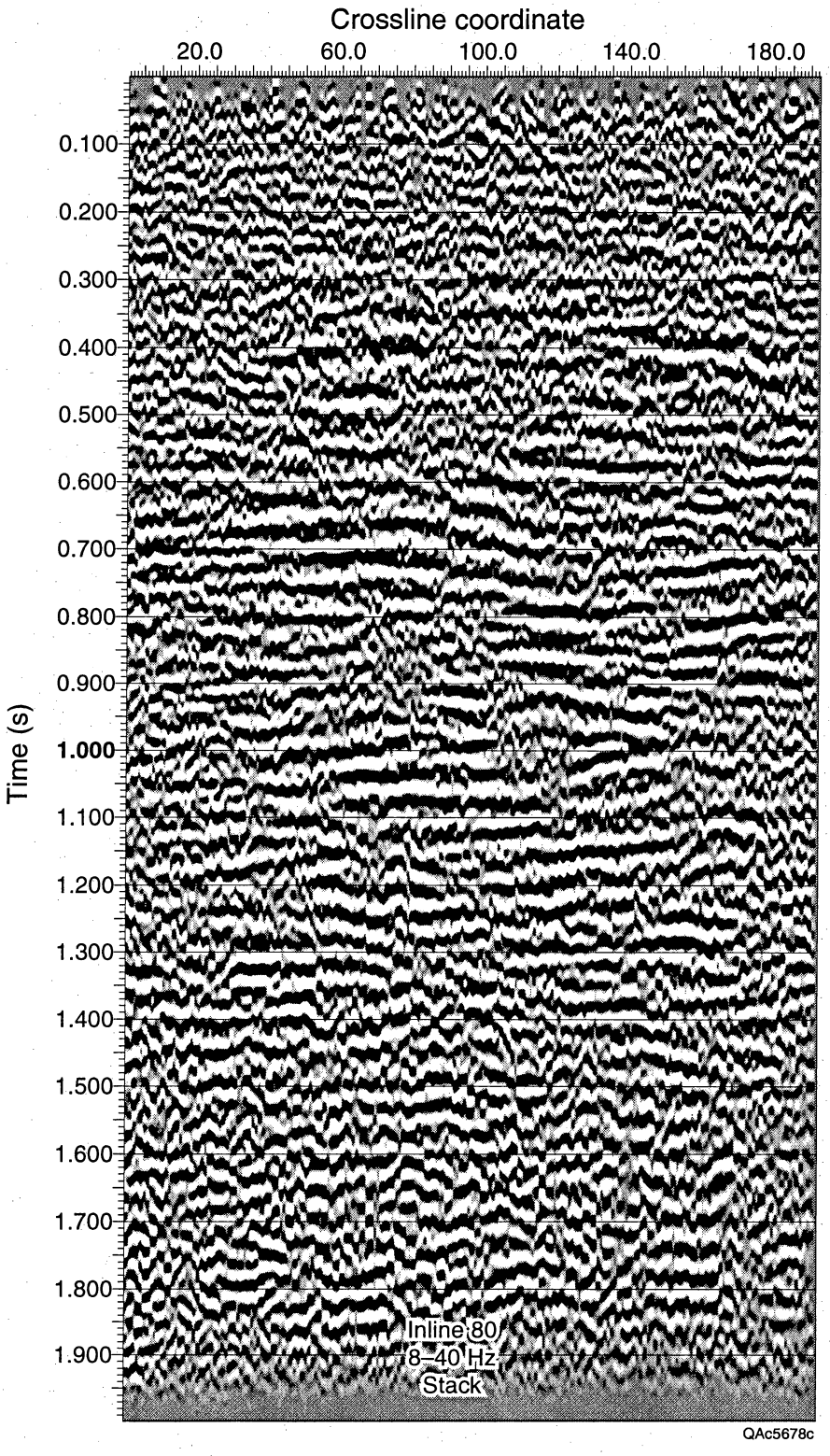

Fig. 30a. Example of vertical section (Inline 80) from the Rye Patch stacked data volume. Line position is shown in Figure 28.

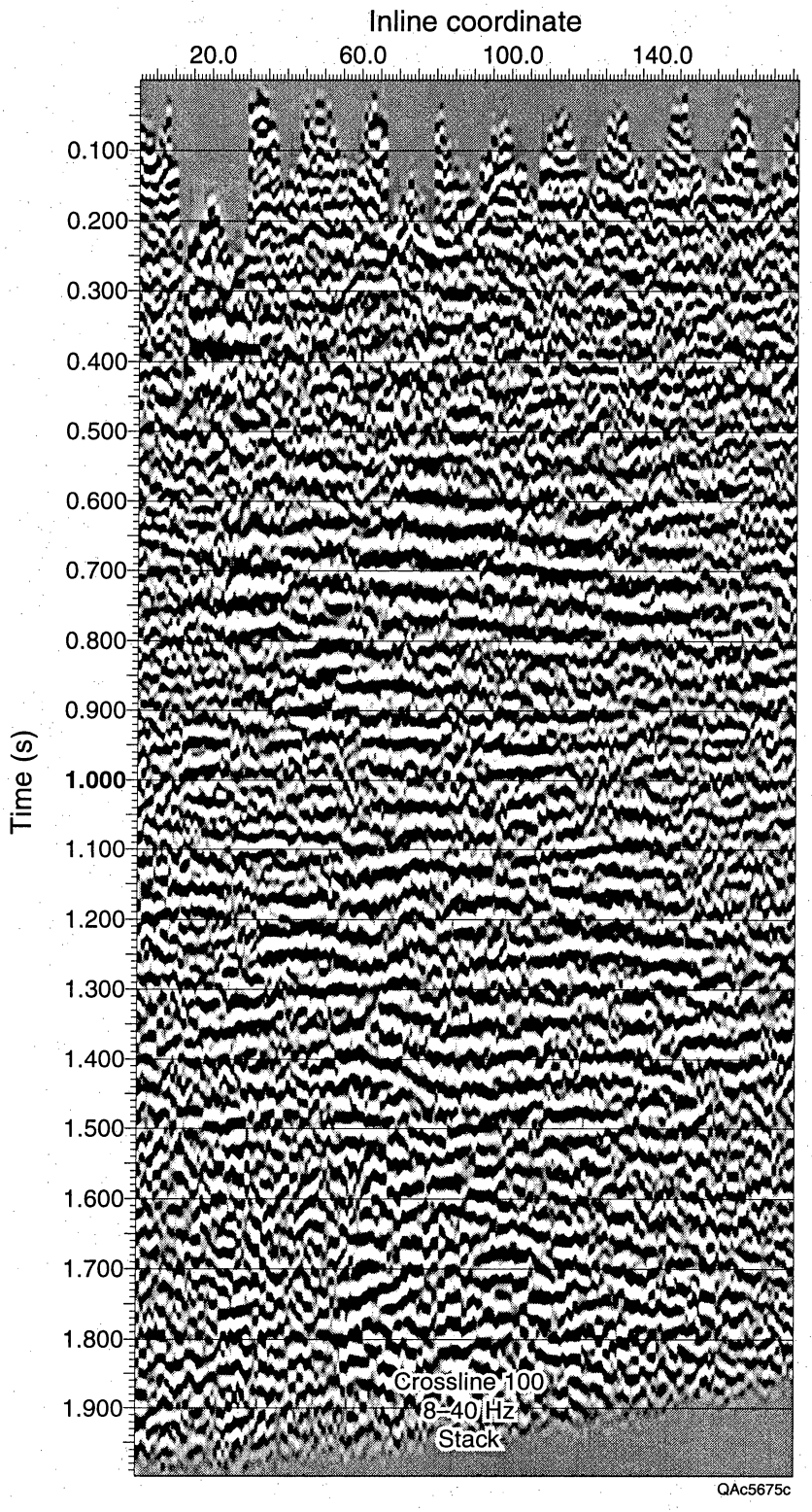

Fig. 30b. Example of vertical section (Crossline 100) from the Rye Patch stacked data volume. Line position is shown in Figure 28.

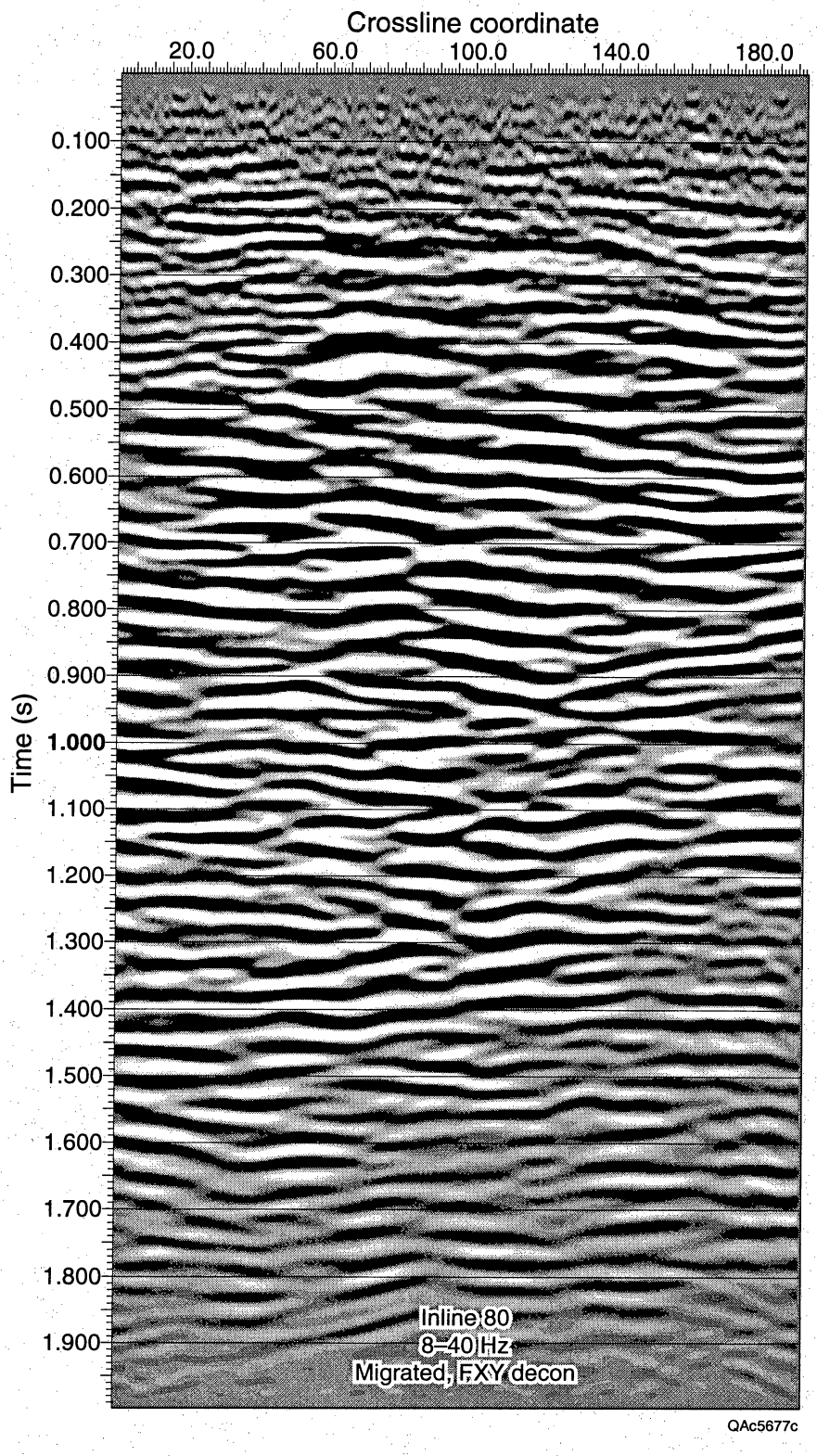

Fig. 31a. Example of vertical section from the Rye Patch migrated data volume. Inline 80 with 8-40 Hz bandwidth.

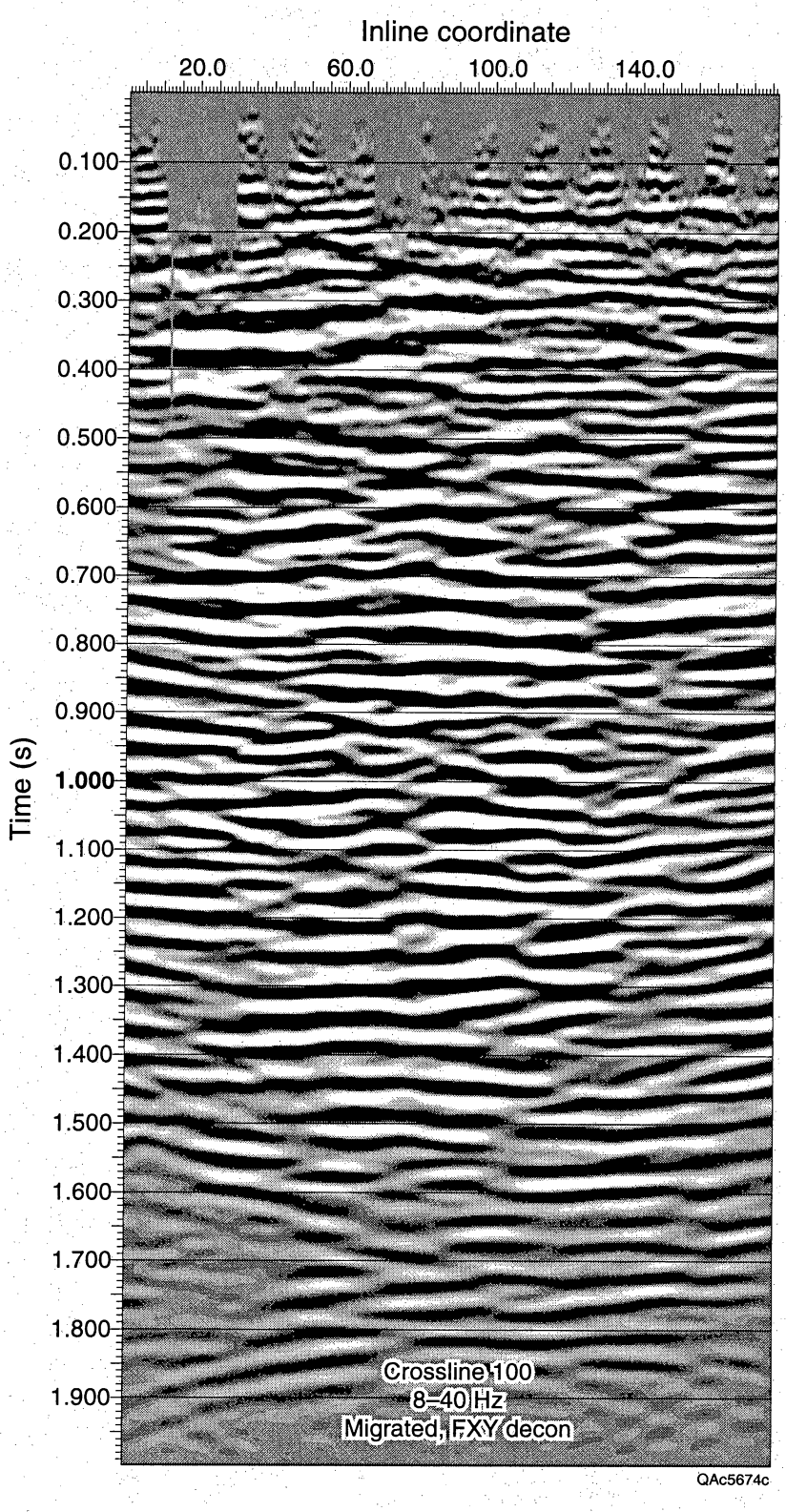

Fig. 31b. Example of vertical section from the Rye Patch migrated data volume. Crossline 100 with 8-40 Hz bandwidth.

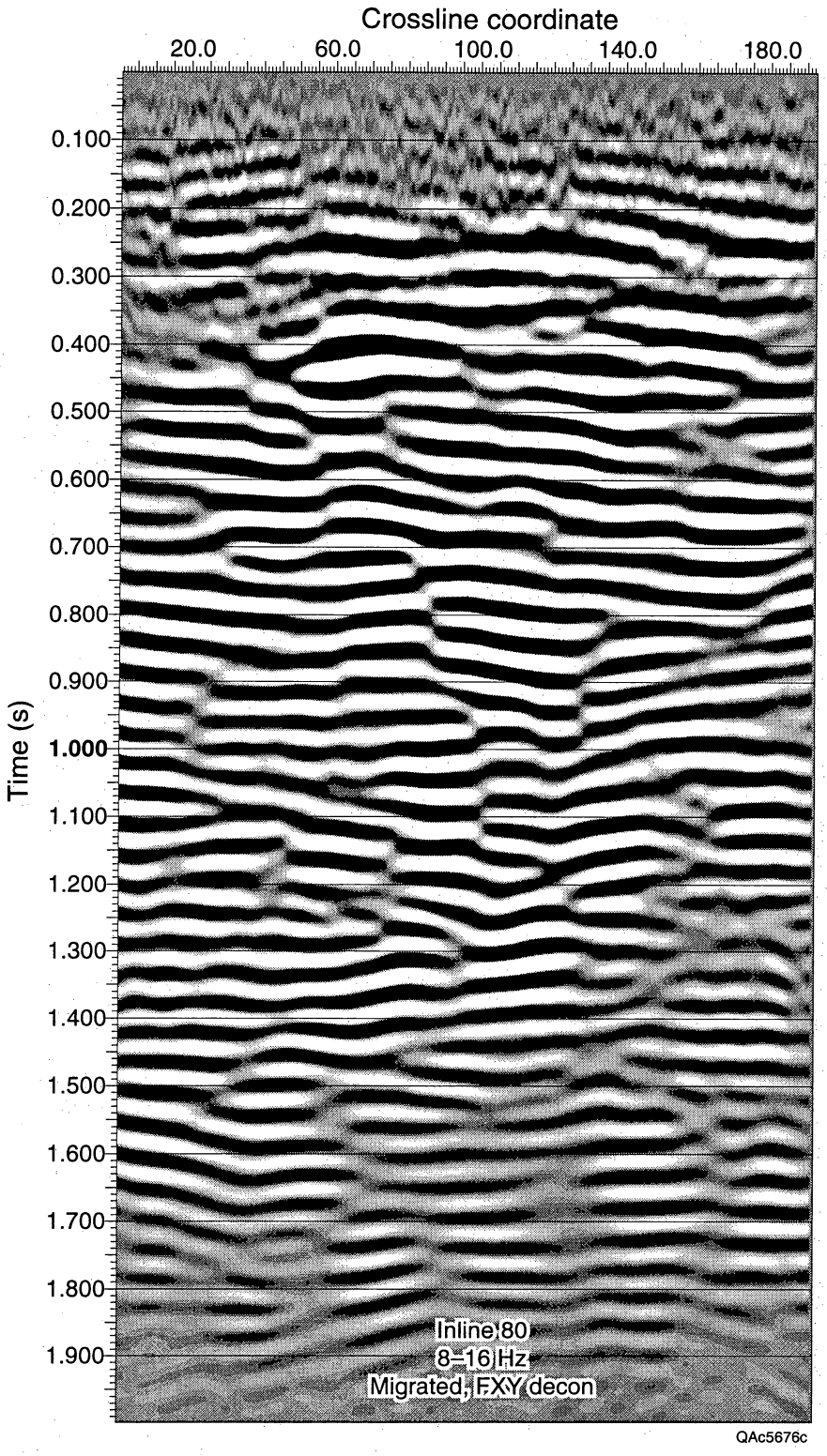

Fig. 31c. Example of vertical section from the Rye Patch migrated data volume. Inline 80 limited to first octave (8-16 Hz).

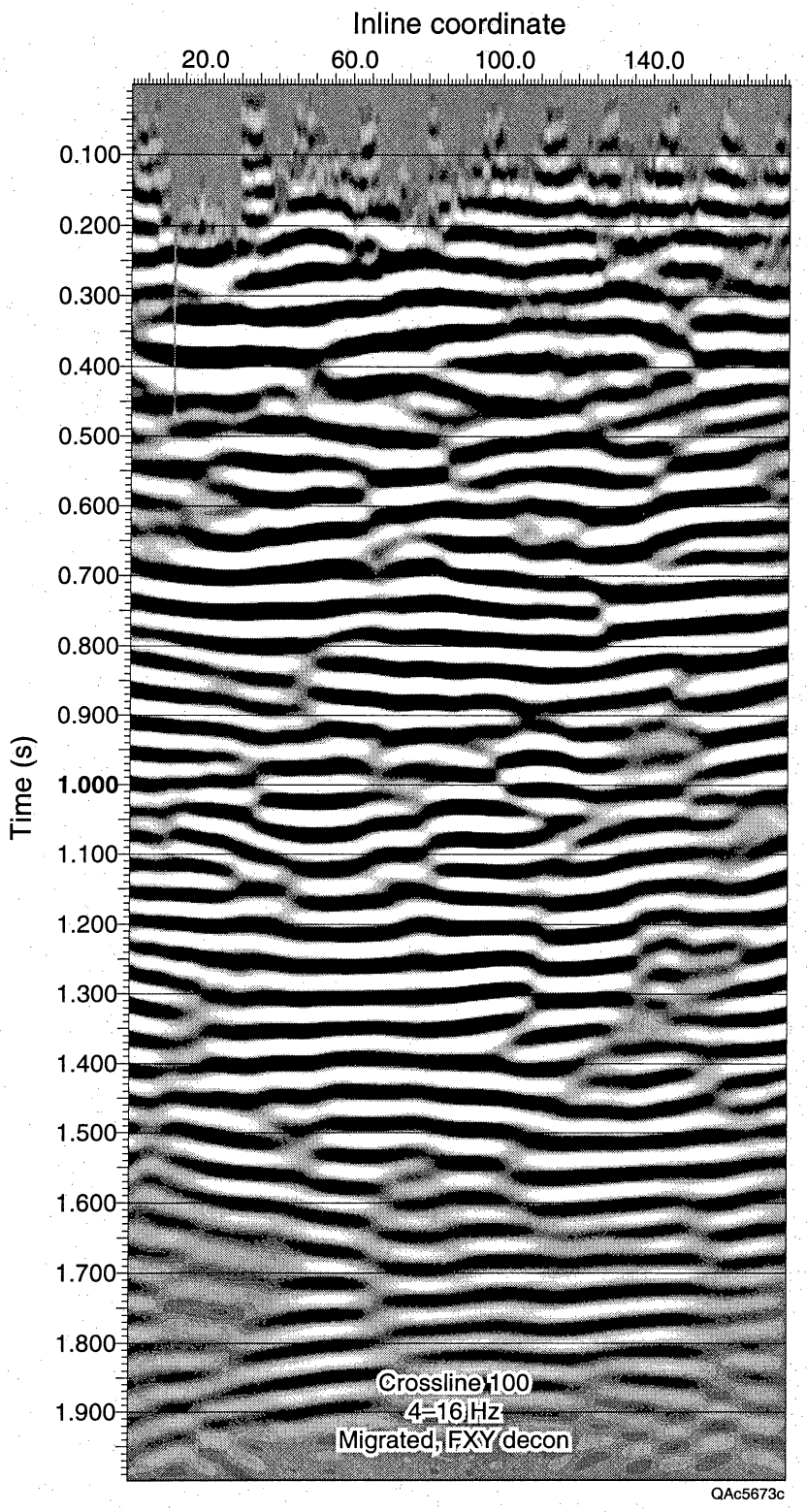

Fig. 31d. Example of vertical section from the Rye Patch migrated data volume. Crossline 100 limited to first octave (8-16 Hz).